Physics of Life

PHYS-468

ATP Synthase

Henning Stahlberg,
LBEM, IPHYS, SB, EPFL

ITAIPU

5 km long
220 m height, 118 m hydraulic height,
20 turbines with 700 m³/s of water flow,
giving 700 MW each,

Output Power = 14 GW
produces
25% of Brasil‘s and almost
100% of Paraguay‘s electricity.

ITAIPU's Turbine

Assembly of the turbine

Schematic drawing of turbine and generator

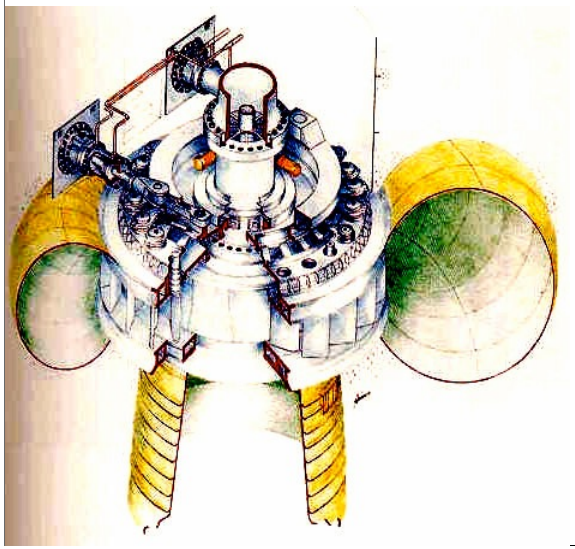

Waterflow * Waterforce

↓

Current * Tension

Turbine from inside the water channel

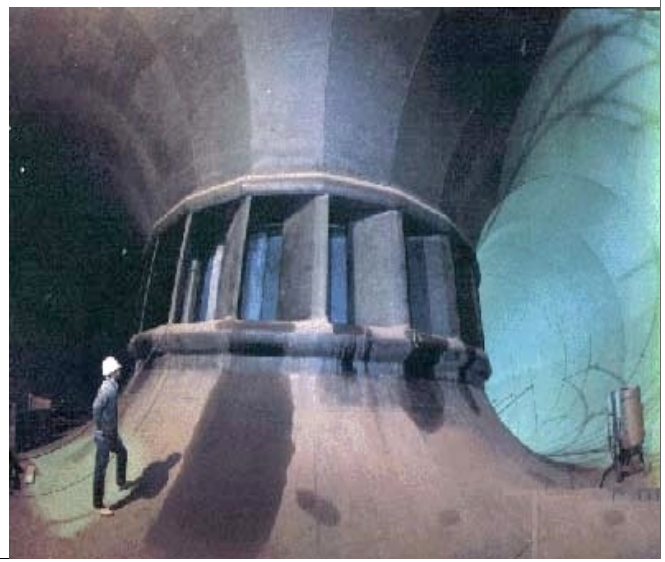

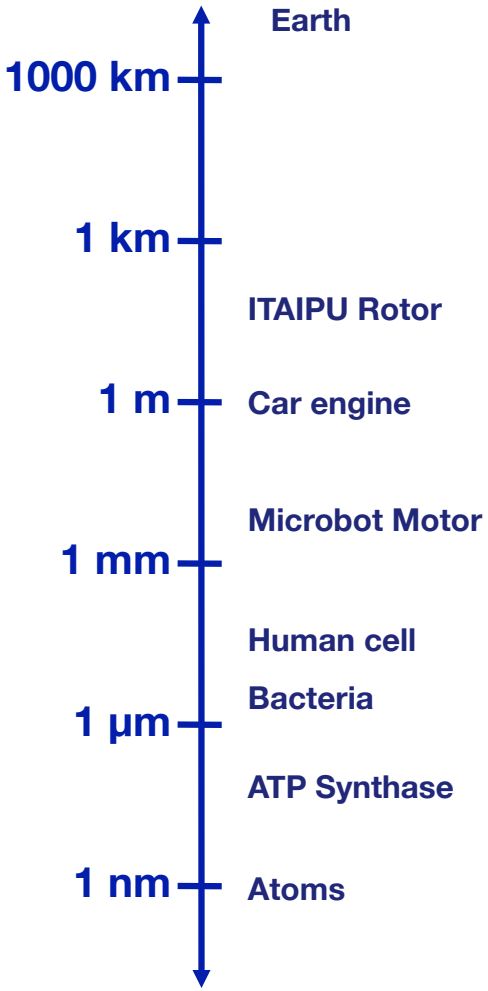

Sandia Microbot:

One of the smallest robots of the world

Photosynthesis in Plant Leaves

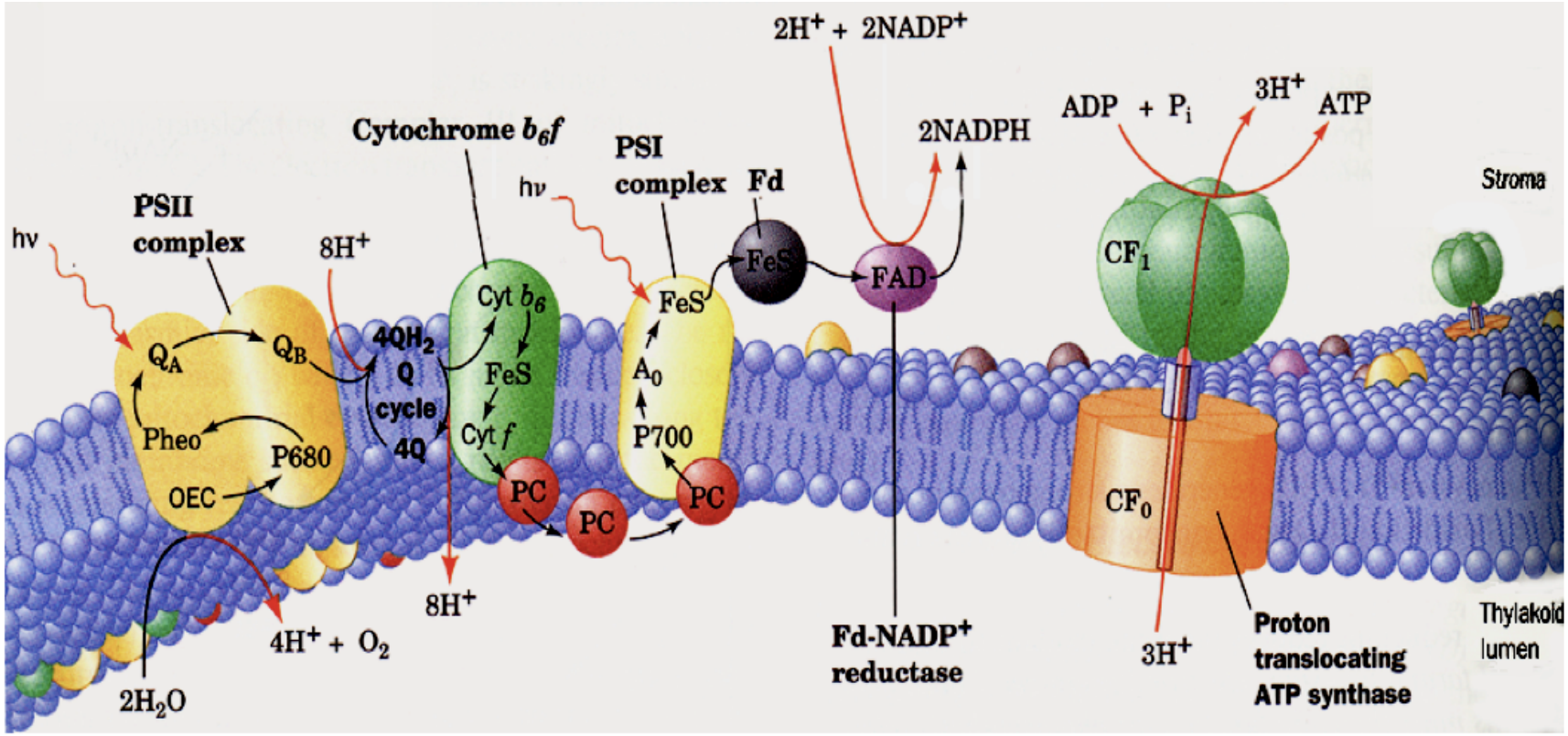

from Voet & Voet, Biochemistry

The Respiratory Chain in Mitochondria

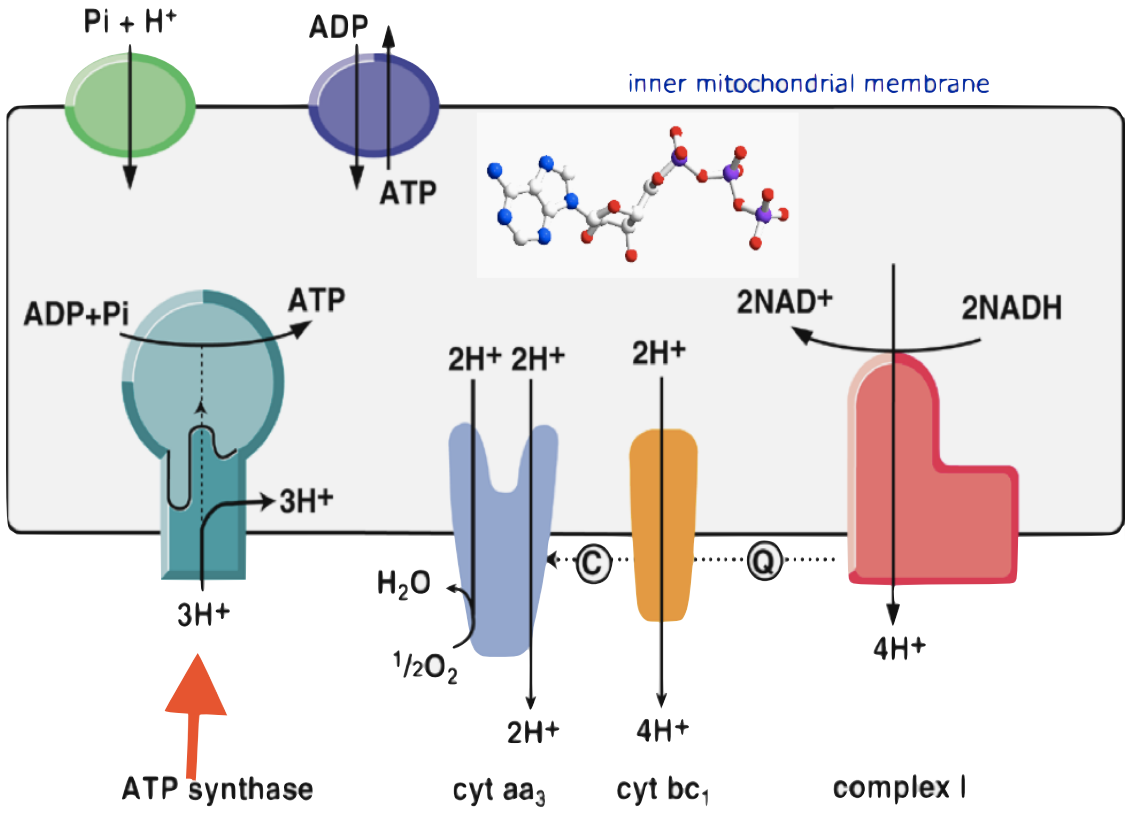

Adenosine Tri-Phosphate

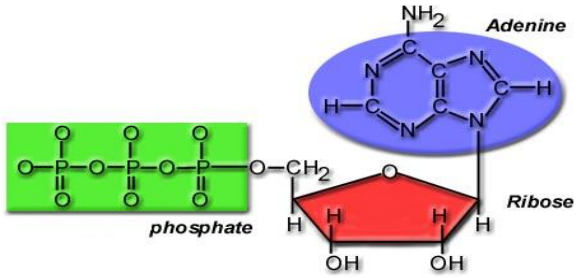

Structure and function of mitochondrial membrane protein complexes

Werner Kühlbrandt

BMC Biology 2015 **13**:89 | **DOI:** 10.1186/s12915-015-0201-x |

Electron Tomography of a Mouse Heart Mitochondrion

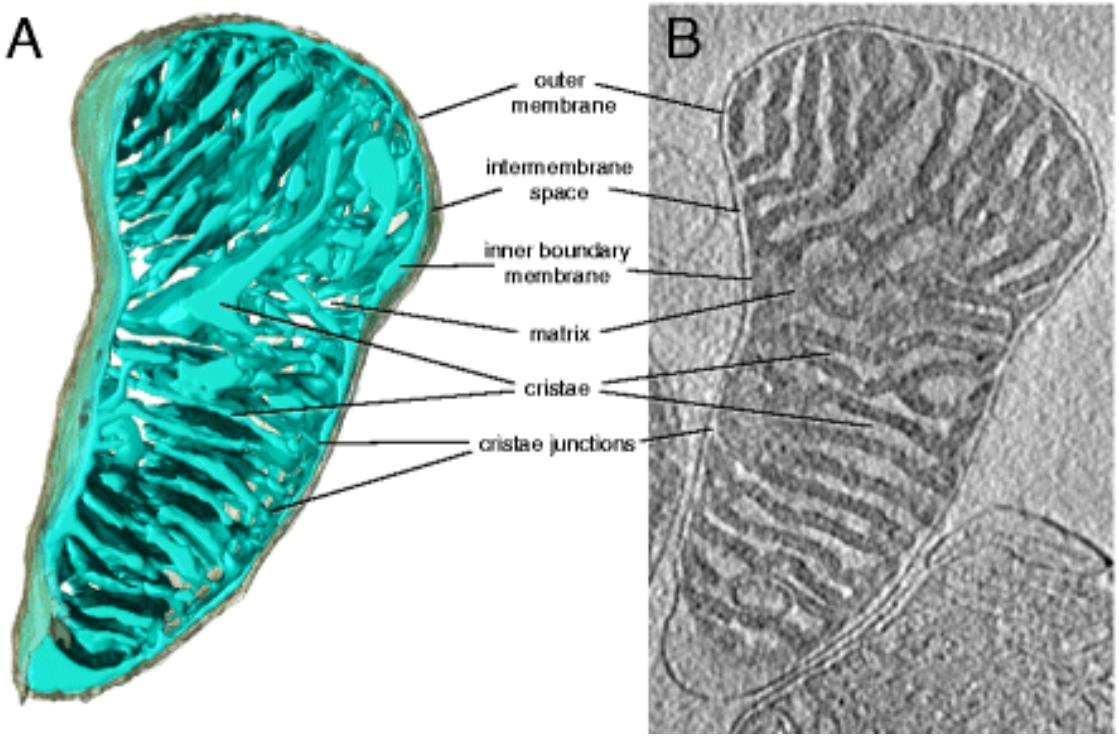

Membrane compartments in the mitochondrion

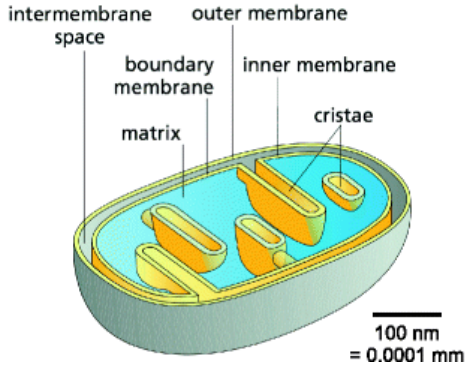

Structure and function of mitochondrial membrane protein complexes

Werner Kühlbrandt

BMC Biology 2015 **13**:89 | **DOI:** 10.1186/s12915-015-0201-x

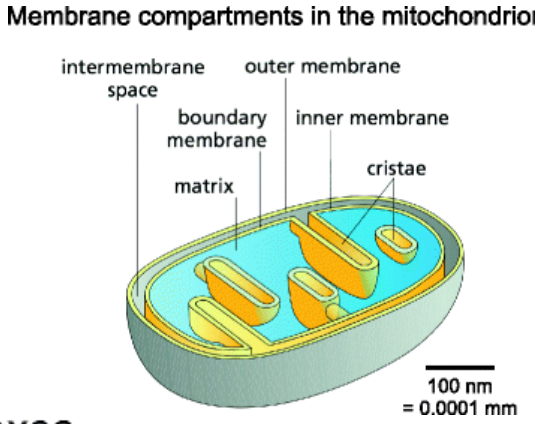

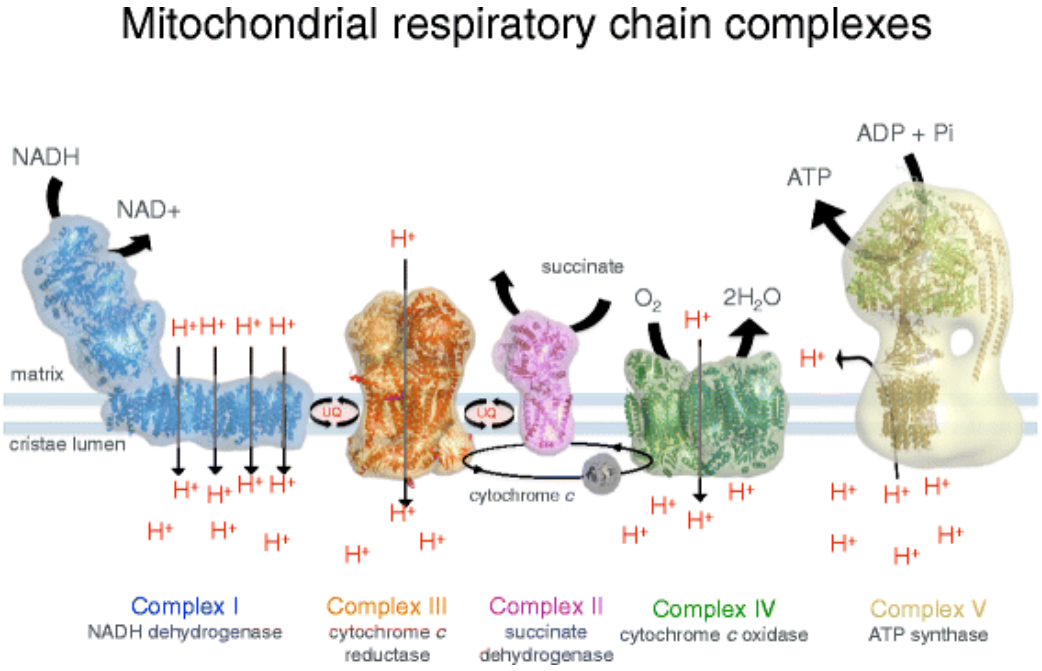

the F1F0 ATPase from *S. cerevisiae*

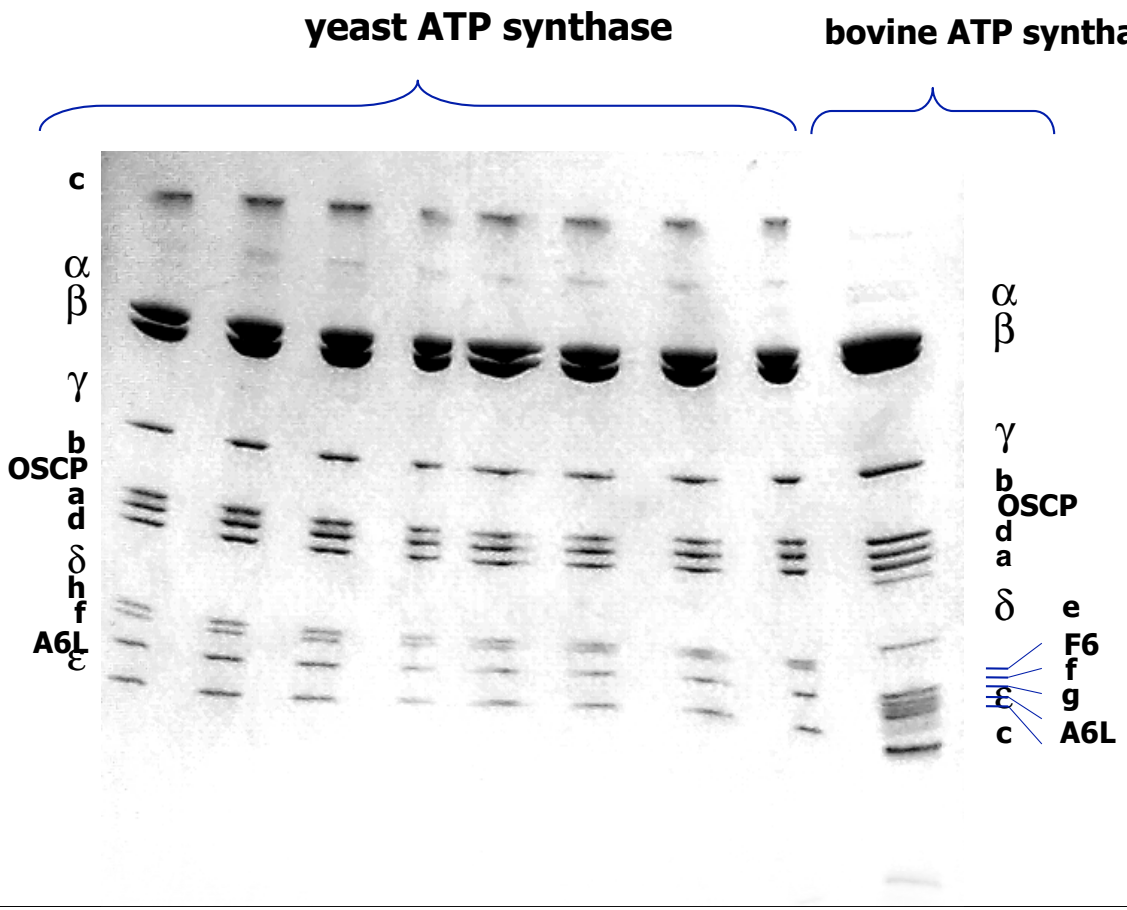

- Cell disruption with bead-beater
- Preparation of yeast mitochondria
- Solubilisation using dodecylmaltoside
- Q-Sepharose
- Gelfiltration

ATP Synthase in synthetical “cell“

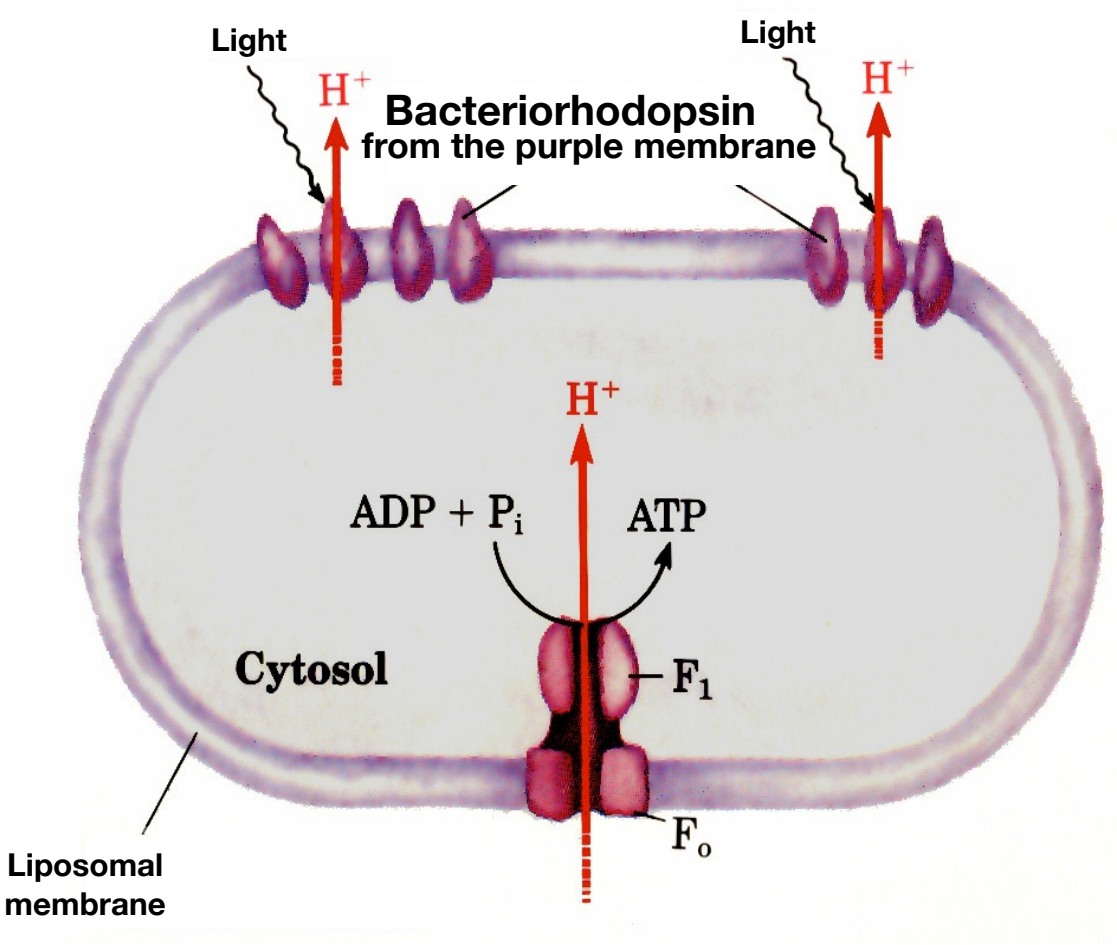

Racker & Stoeckenius, J. Biol. Chem. 249 (1974)

ATP-Synthesis

$$ADP^{3-}{}_i + HPO_4{}^{2-}{}_i + H^+{}_i \rightarrow ATP^{4-}{}_i + H_2O_i$$

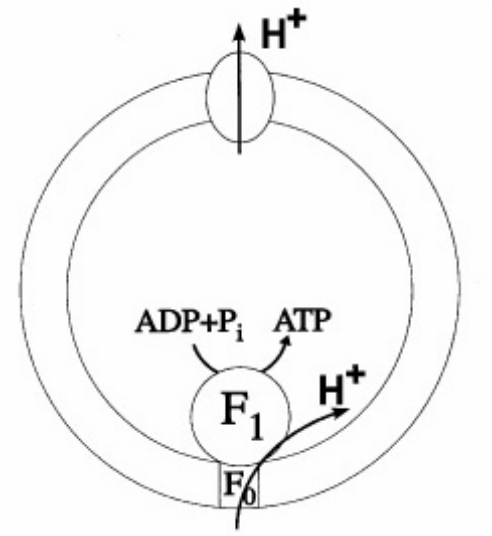

ATP-Hydrolysis

$$ATP^{4-} + H_2O \rightarrow ADP^{3-} + HPO_4{}^{2-} + H^+$$

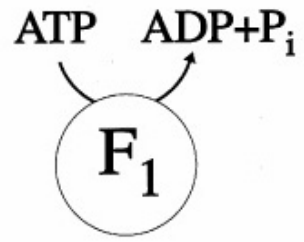

First TEM images of the ATP Synthase

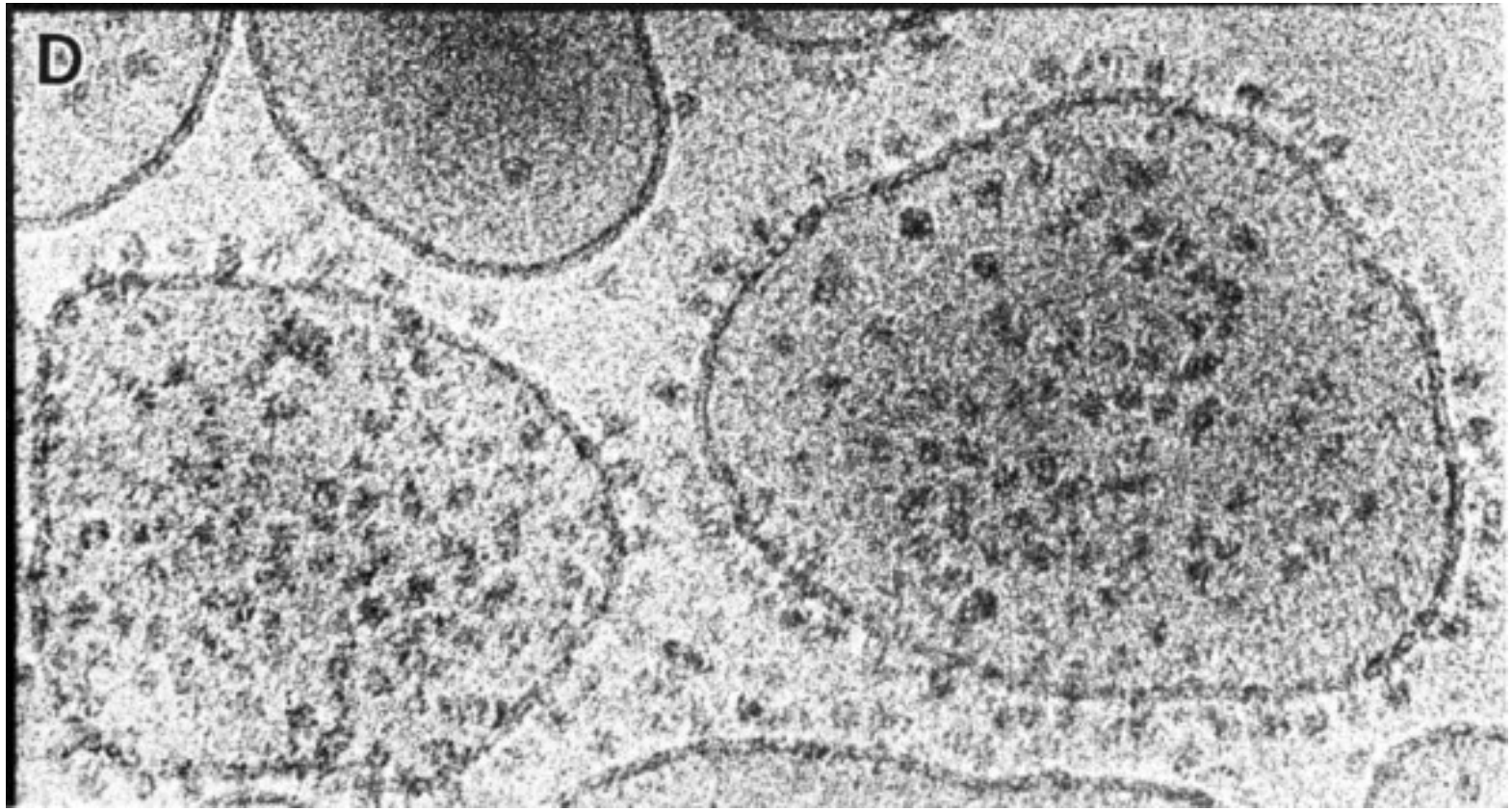

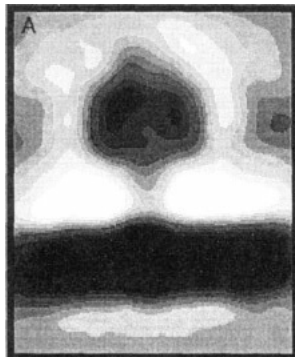

Gogol *et al.*, FEBS Lett. 1987

TEM images of negatively stained ATP Synthase

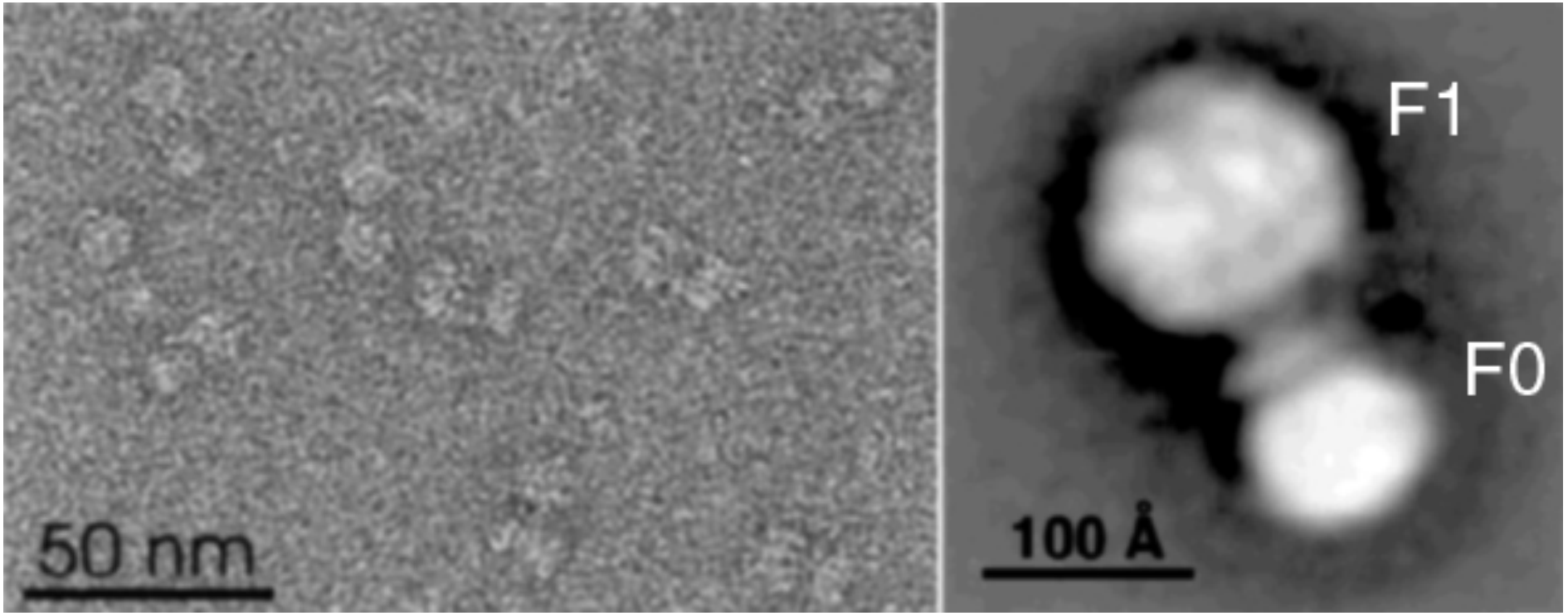

Karrasch & Walker, 1999

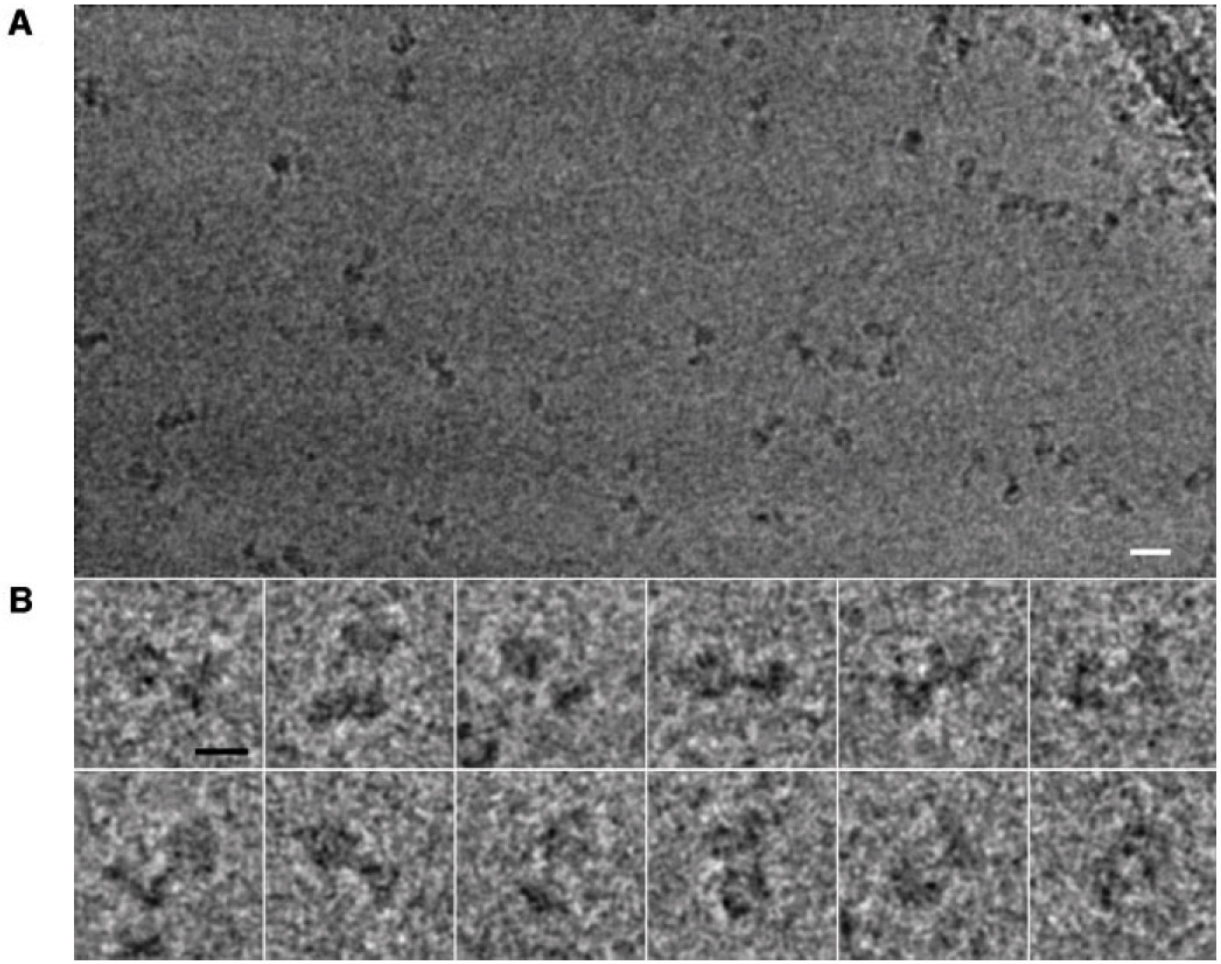

Fig. 1. EM of ATP synthase particles. Frozen ATP synthase particles were imaged with a 200 kV electron microscope. (**A**) A sample region from a micrograph. (**B**) Some typical particle images. The scale bar in (A) represents 200 Å and the scale bar in (B) represents 100 Å.

Rubinstein, Walker, Henderson, EMBO J., 2003

J.L.Rubinstein, J.E.Walker and **R.Henderson**

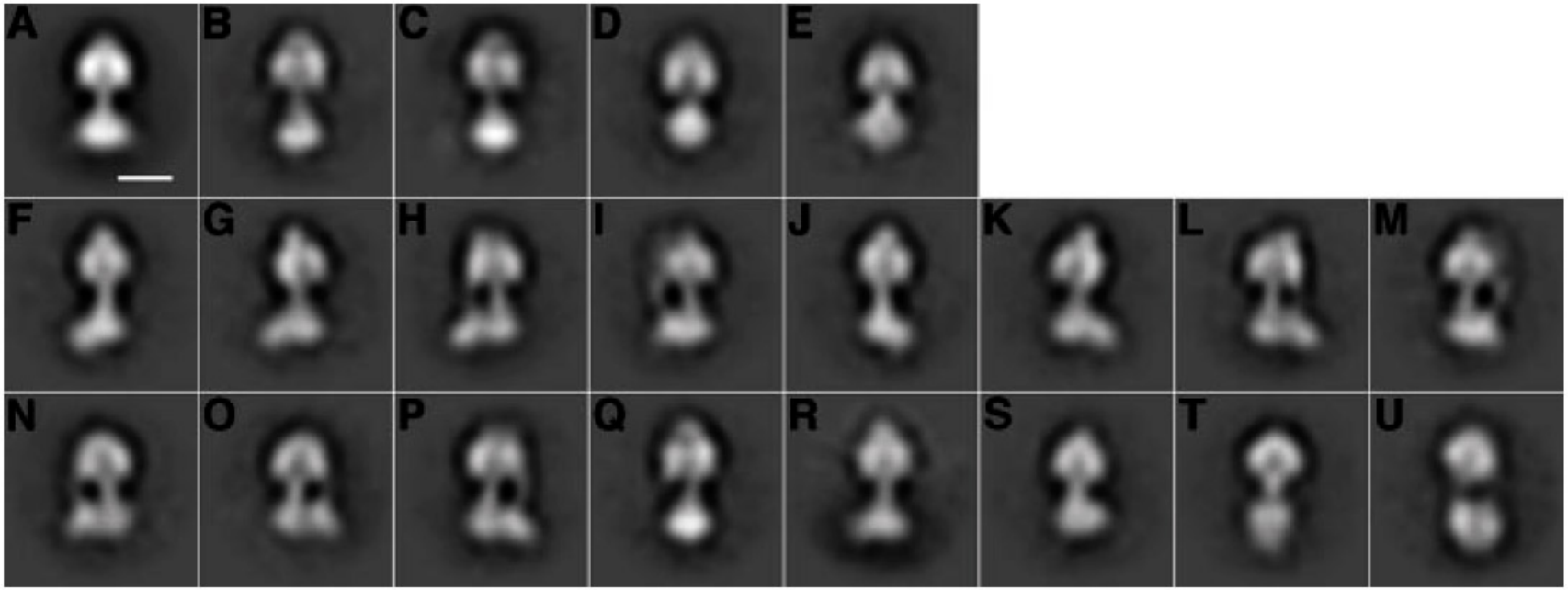

Fig. 2. Class-average images of the ATP synthase. (**A**) Average of all of the aligned images in the dataset. The scale bar represents 100 Å. (**B**–**E**) Class-averages that probably arise from incoherently averaged particle images (and consequently, like the overall average, have a line of symmetry). (**F**–**M**) Class-averages where a corresponding mirror image is found (e.g. F with J, G with K, etc.) and constitute views about the long axis of the complex. (**N** and **O**) A mirror pair, but each probably consisting of averages of two non-equivalent views of the assembly with the long axis tilted from the plane of the grid. (**P**–**U**) Class averages that have no mirror pair in the dataset.

Rubinstein, Walker, Henderson, EMBO J., 2003

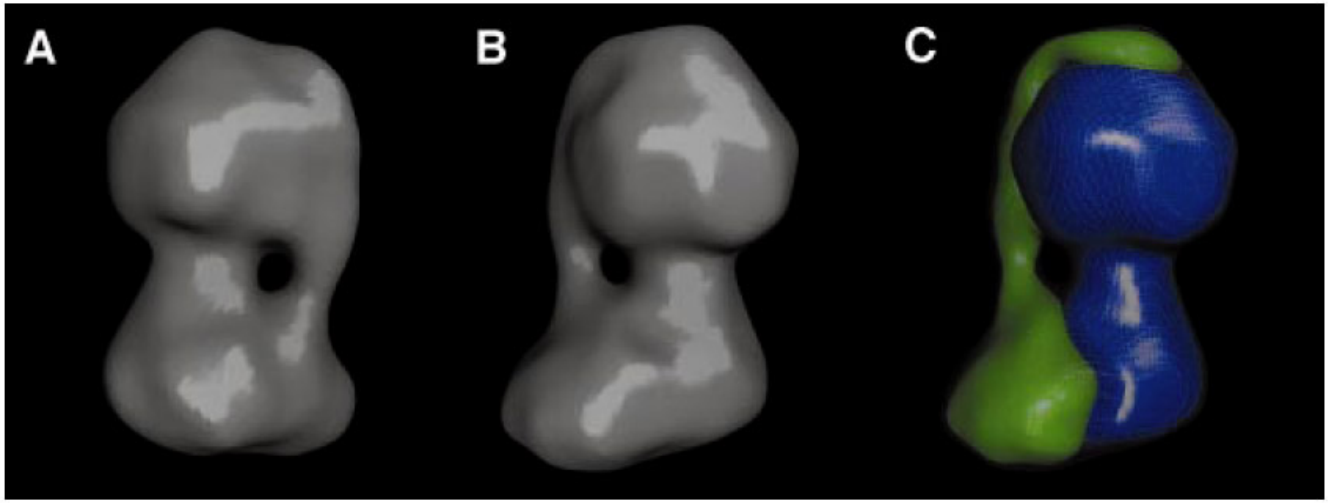

Fig. 4. 3-D model of the ATP synthase. (**A** and **B**) Surface rendered views of the model after refinement. (**C**) The model after being divided into two parts. The first (blue) was chosen to correspond to the F_1-c_{10} subcomplex and the remaining density (green) is interpreted to represent the peripheral stalk and second domain of F_O. The grey mesh represents the experimental EM map.

Rubinstein, Walker, Henderson, EMBO J., 2003

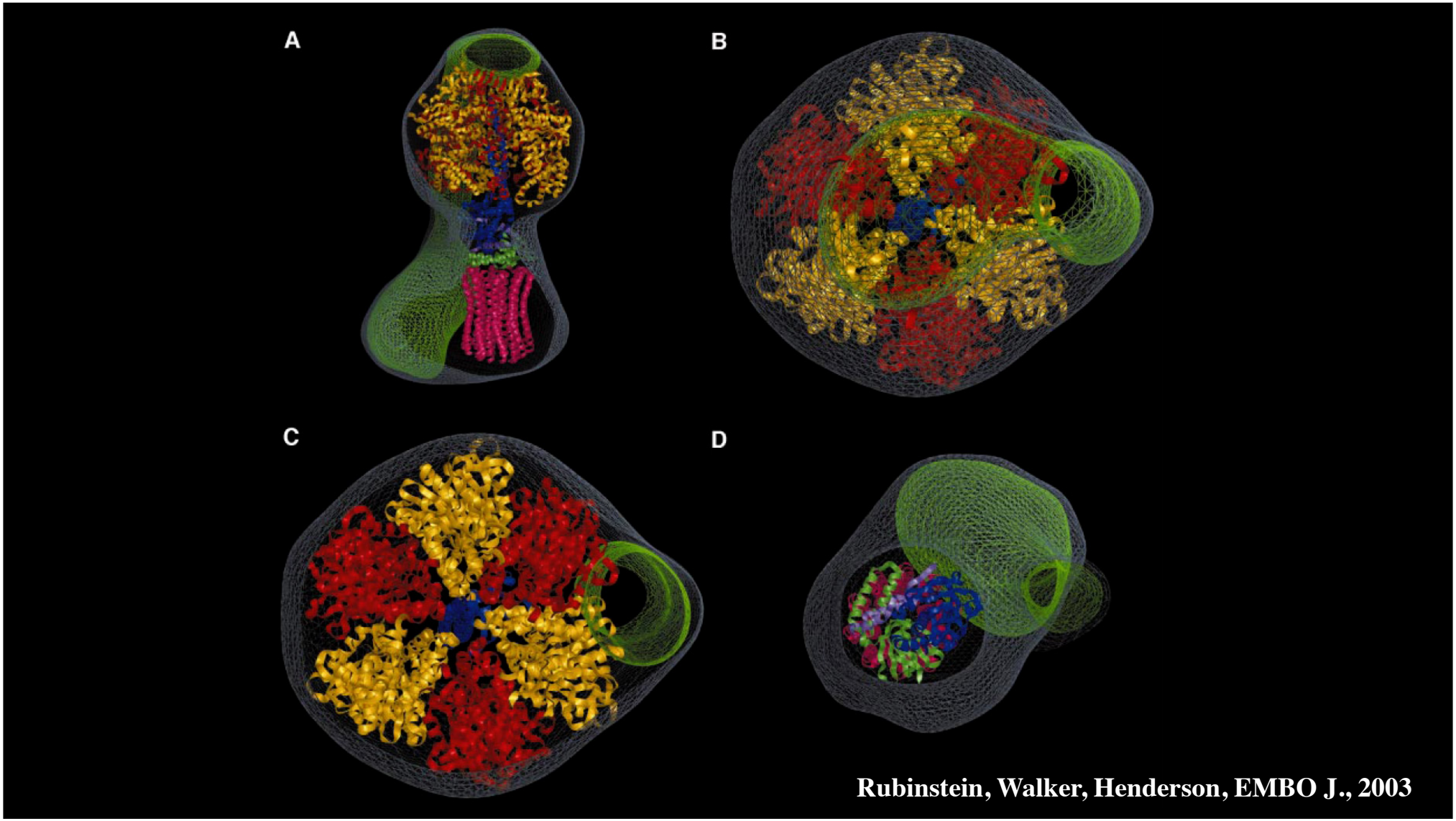
A
B
C
D
Rubinstein, Walker, Henderson, EMBO J., 2003

LETTER

doi:10.1038/nature10699

Subnanometre-resolution structure of the intact *Thermus thermophilus* H^+-driven ATP synthase

Wilson C. Y. Lau[1,2] & John L. Rubinstein[1,2,3]

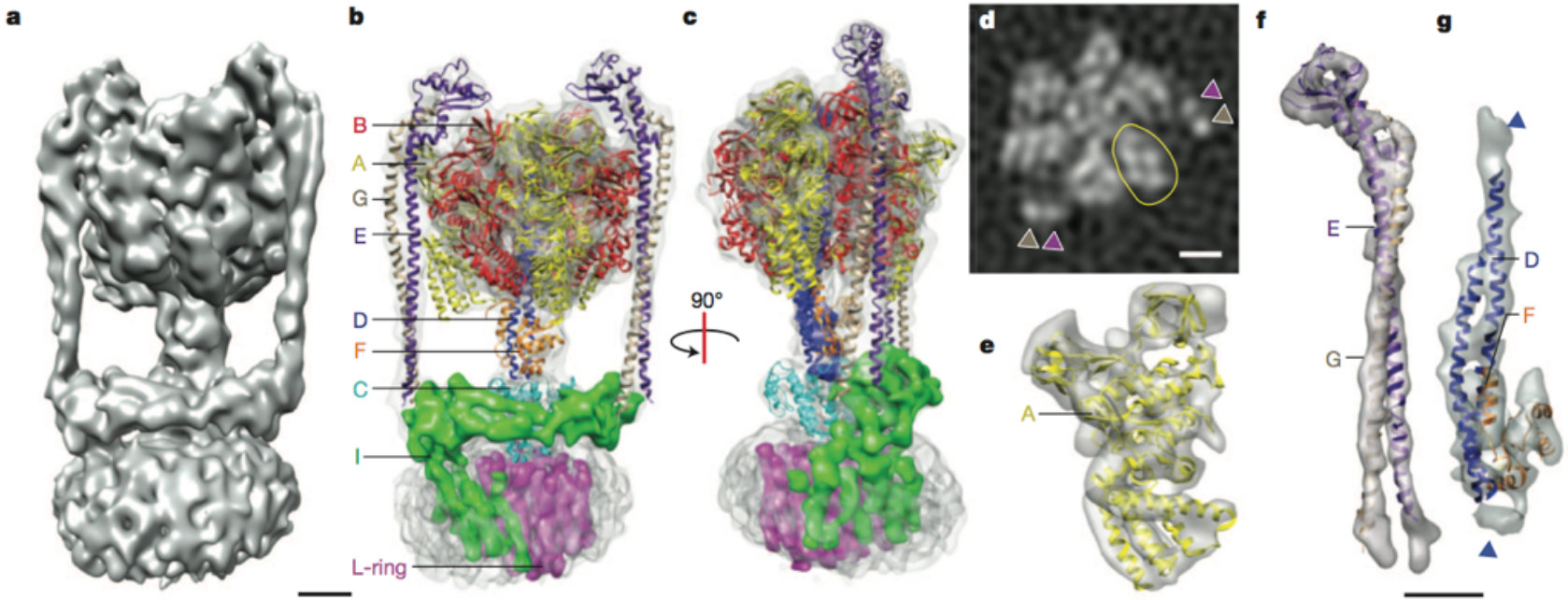

Figure 1 | Three-dimensional map of the *T. thermophilus* ATP synthase. **a**, A surface view of the three-dimensional map. **b**, **c**, The overall map (semi-transparent grey) with fitted crystal structures and segments corresponding to individual subunits. Segments of the cryo-EM map are shown for the L_{12} ring, subunit I and residues of subunit D missing from its crystal structure. **d**, A cross-section through the soluble region of the map shows that α-helices from the two E subunits (purple arrows) and two G subunits (beige arrows) can be resolved. Helices can also be resolved in other subunits, such as the A subunits (example circled in yellow). The map segments agree with crystal structures, such as subunit A (**e**), the EG subcomplex (**f**) and the DF subcomplex (**g**). Density corresponding to missing residues from the crystal structure of the D subunit is indicated with blue arrows. Scale bars, 25 Å.

LETTER

214 | NATURE | VOL 481 | 12 JANUARY 2012

doi:10.1038/nature10699

Subnanometre-resolution structure of the intact *Thermus thermophilus* H^+-driven ATP synthase

Wilson C. Y. Lau[1,2] & John L. Rubinstein[1,2,3]

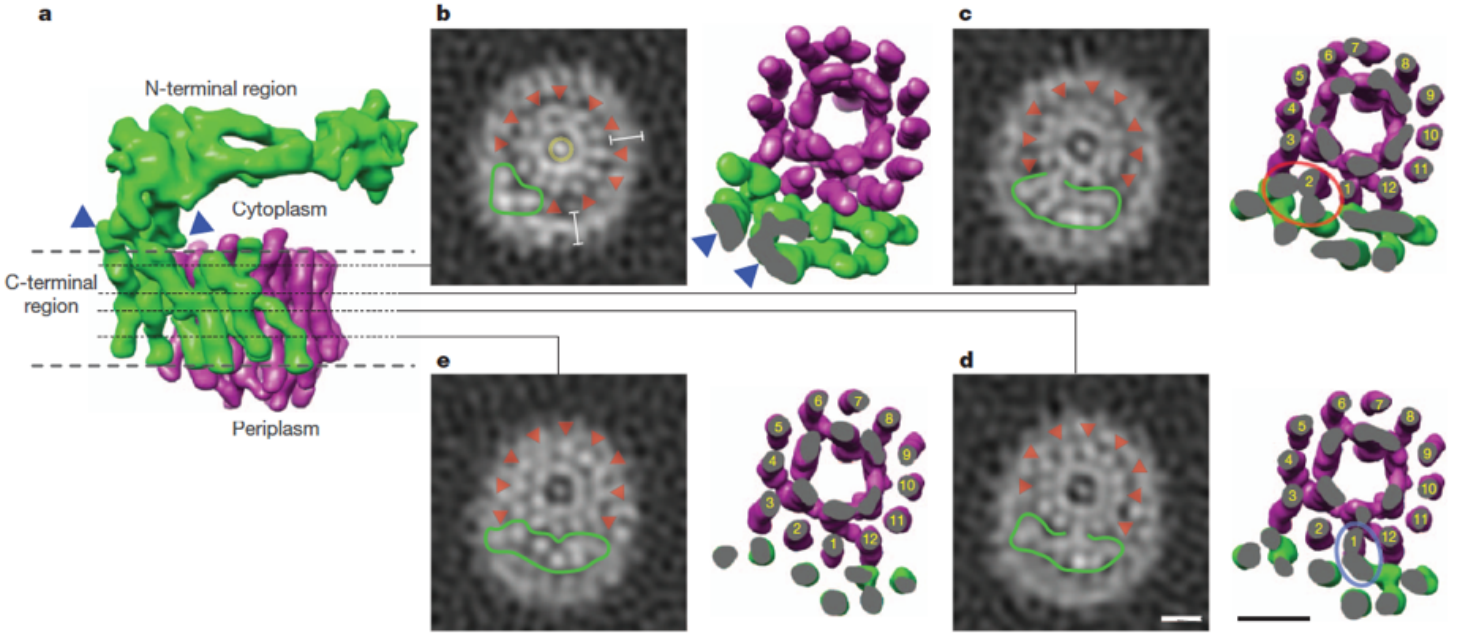

Figure 3 | The membrane-bound region of the enzyme. **a**, Map segments of the L_{12} ring (magenta) and subunit I (green) showing multiple contacts between the N- and C-terminal regions of subunit I (blue arrows). **b**, Cross-sections through the map (left panel) and map segments truncated at the same height (right panel) show subunit I separated from the L_{12} ring near the cytoplasm. Outer helices of the L_{12} ring are indicated (red arrows) and the transmembrane helices of subunit I are outlined (green). Cross-sections show the detergent micelle (white bars) and detergent or lipid in the centre of the L_{12} ring (yellow circle). **c**, Near the middle of the membrane, subunit I contacts an L subunit, probably forming the mid-membrane end of the cytoplasmic half channel (circle in red in right panel). **d**, Approximately 6 Å further towards the periplasm subunit I contacts a different L subunit, probably forming the mid-membrane end of the periplasmic half-channel (circled in blue in right panel). **e**, Subunit I is separated from the L_{12} ring near the periplasm. Scale bars, 25 Å.

E. coli EF_OEF_1 - ATPase (in year 2000)

EF_1

$\alpha_3\beta_3\gamma\delta\varepsilon$
381 kDa

EF_OEF_1: 541 kDa

EF_O

$ab_2c_{10\text{-}14}$
160 kDa

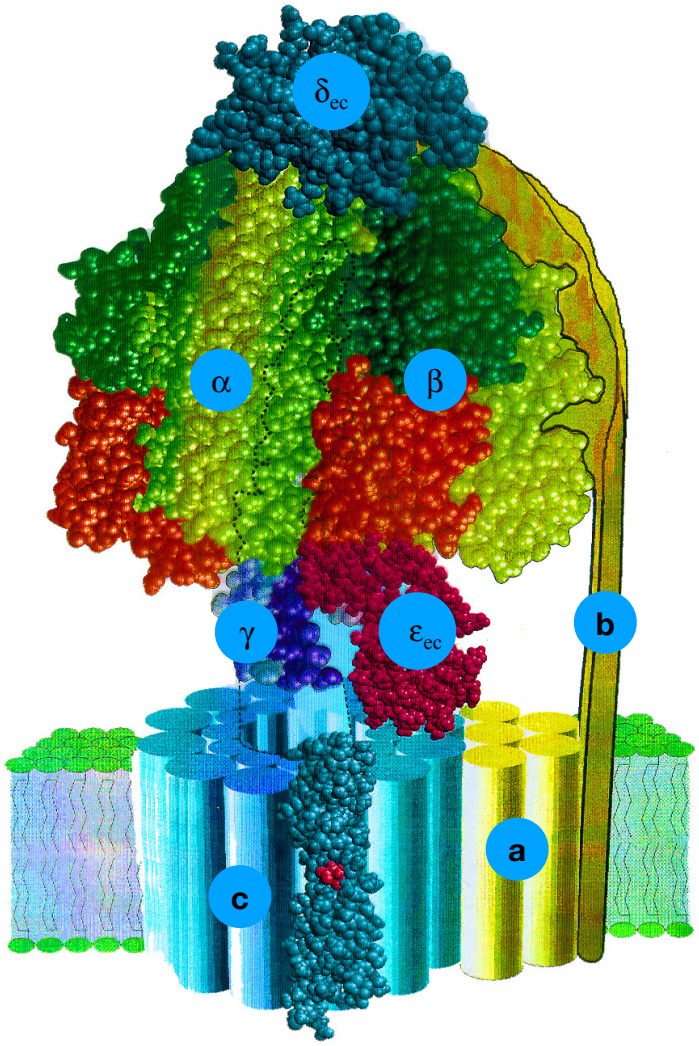

adapted from Sigfried Engelbrecht and Wolfgang Junge,

Comparison of bovine/ yeast F1Fo ATPase

subunit	MW [kDa] bovine/yeast	sequence identity/length
alpha	55.2 / 55.3	73% / 507 residues
beta	51.7 / 52.5	79% / 467
gamma	30.1 / 30.6	40% / 277
delta	15.0 / 14.6	34% / 143
epsilon	5.7 / 6.6	39% / 38
b	24.7 / 23.3	24% / 179
OSCP	20.9 / 20.9	34% / 186
d	18.6 / 19.7	22% / 145
a	24.8 / 27.9	34% / 205
e	(8.2 / 10.9)	42% / 43
F6	9.0 / ----	----
f	9.4 / 11.3	25% / 44
h	---- / 14.1	----
g	(11.4 / 12.9)	29% / 105
A6L	8.0 / 5.9	42% / 24
c	7.6 / 7.8	64% / 70
IF1	(9.6 / 9.3)	39% / 46

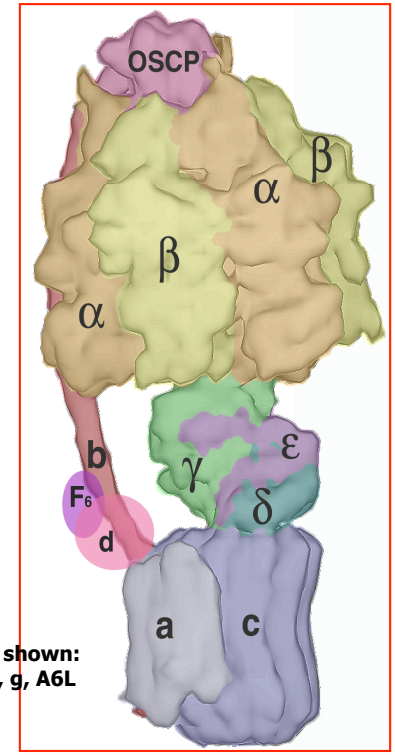

The bovine F1 ATPase

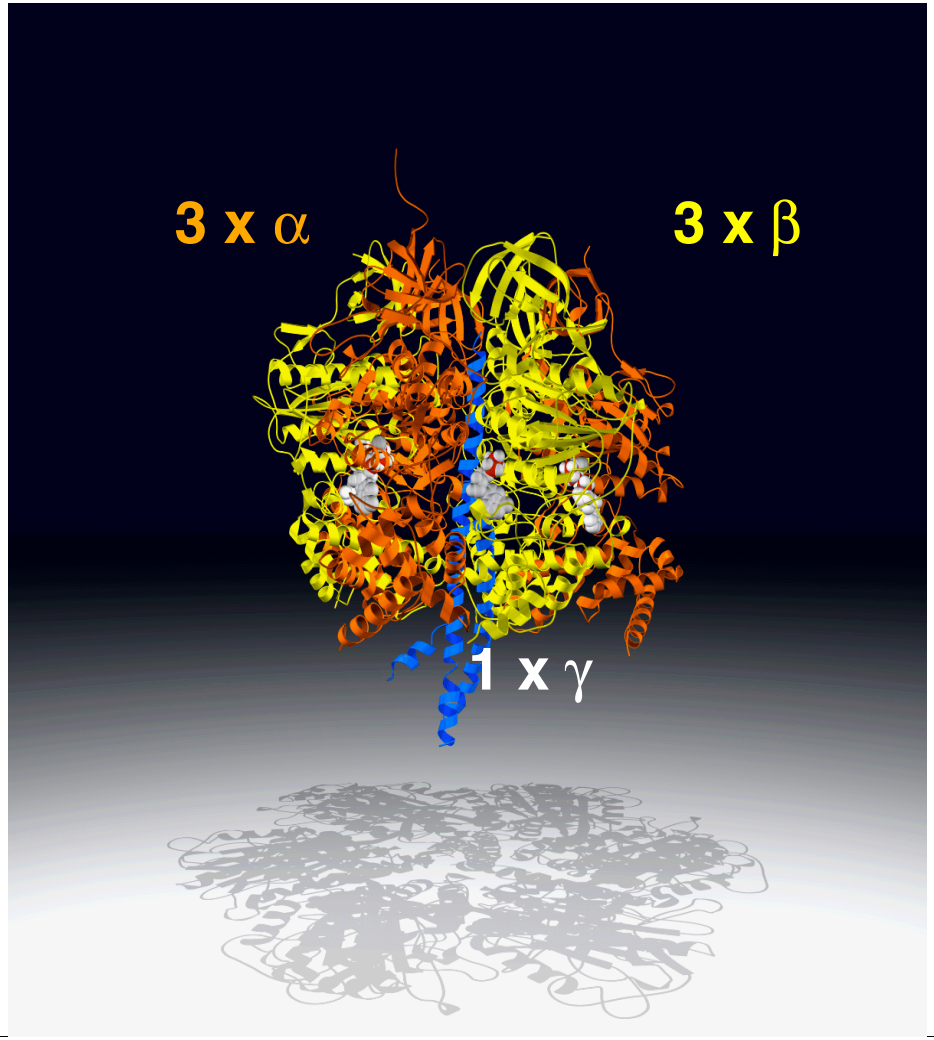

Abrahams et al. (1994) Nature 370, 621

3 x α subunits

3 x β subunits

1 x γ subunit

4 x AMPPNP

1 x ADP

The bovine F1 ATPase

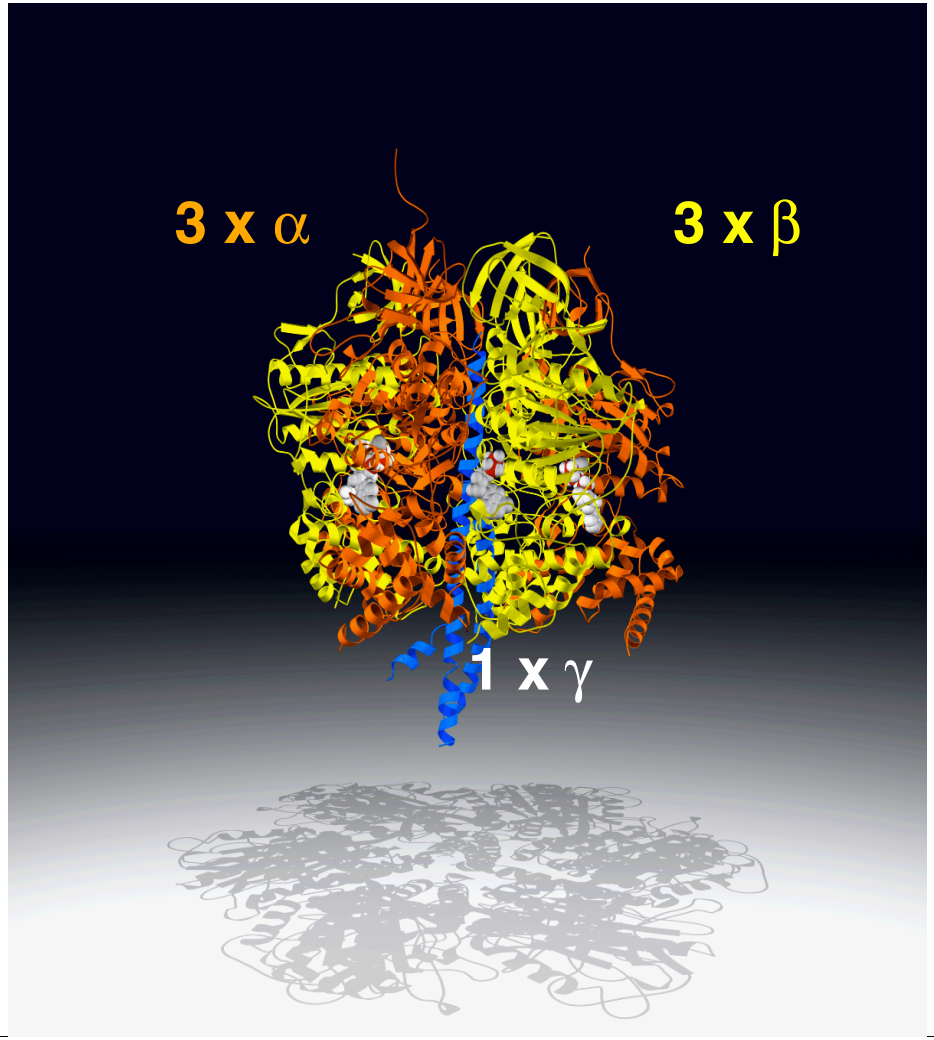

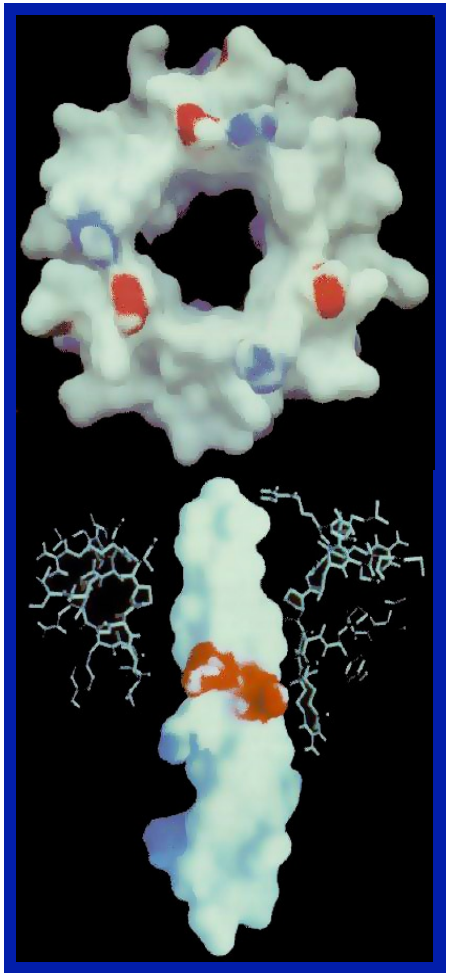

Abrahams *et al.*, Nature 370 (1994)

Boyer's Binding Change Model

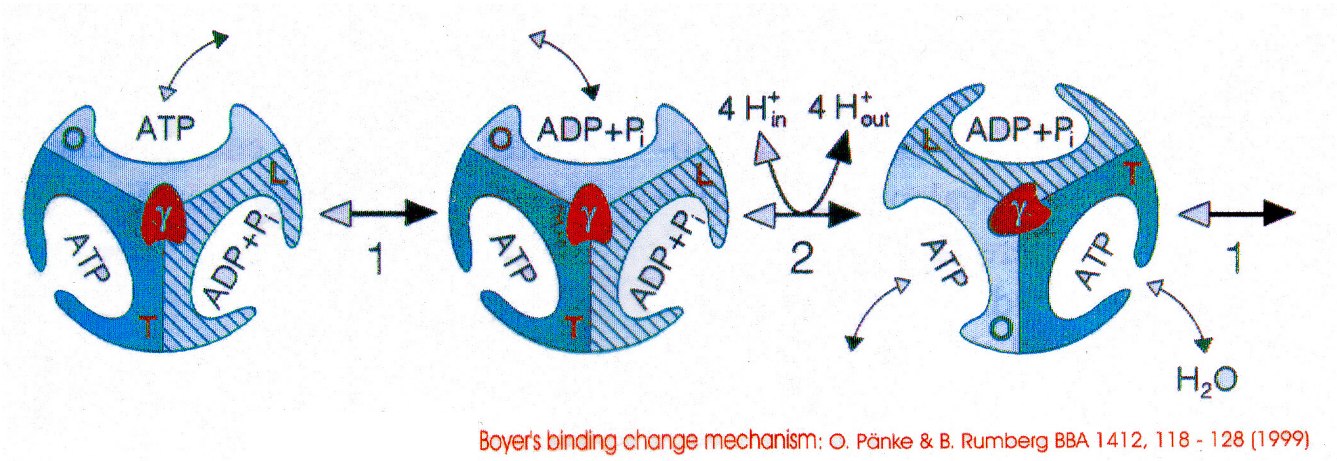

Boyer's binding change mechanism: O. Pänke & B. Rumberg BBA 1412, 118 - 128 (1999)

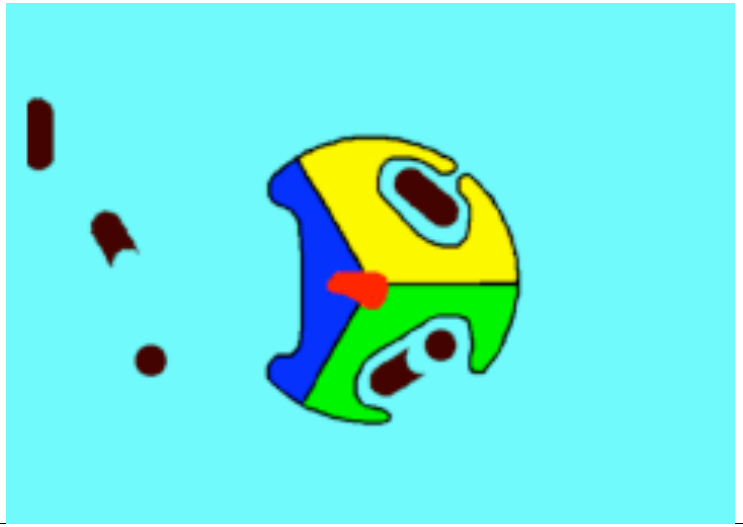

The three-fold symmetric structure of F1

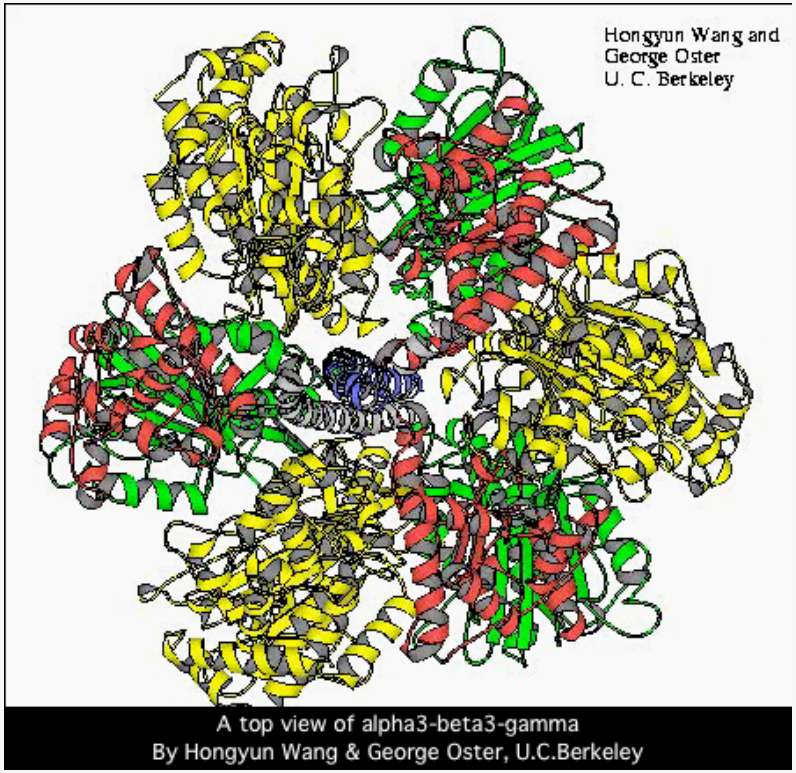

A top view of alpha3-beta3-gamma
By Hongyun Wang & George Oster, U.C.Berkeley

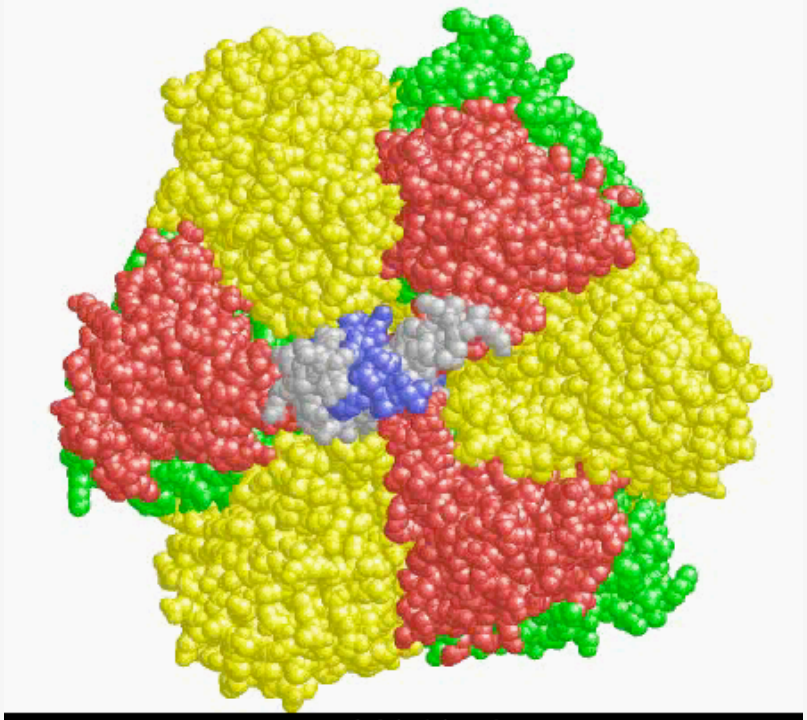

A top view of alpha3-beta3-gamma
By Hongyun Wang & George Oster, U.C.Berkeley

The Walker Domain A and B in Alpha and Beta Subunits form the ATP binding pocket

A cross-section view of alpha-beta-gamma
By Hongyun Wang & George Oster, U.C.Berkeley

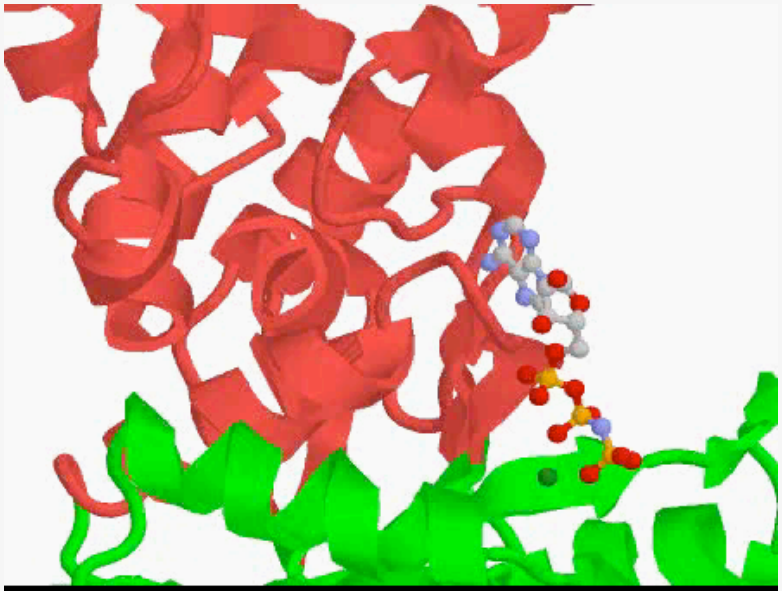
A zoom-in view of beta near the catalytic site
By Hongyun Wang & George Oster, U.C.Berkeley

Direct Observation of Rotation

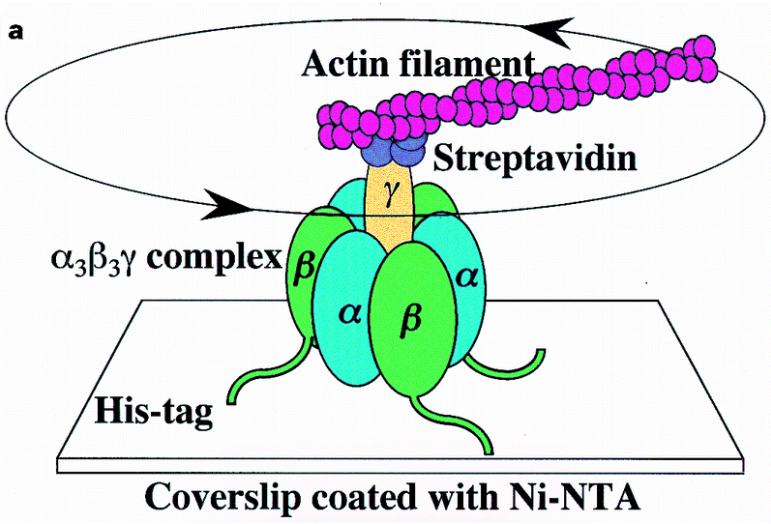

H. Noji, M. Yasuda, M. Yoshida, K. Kinosita, (1997) Nature 386, p. 299.

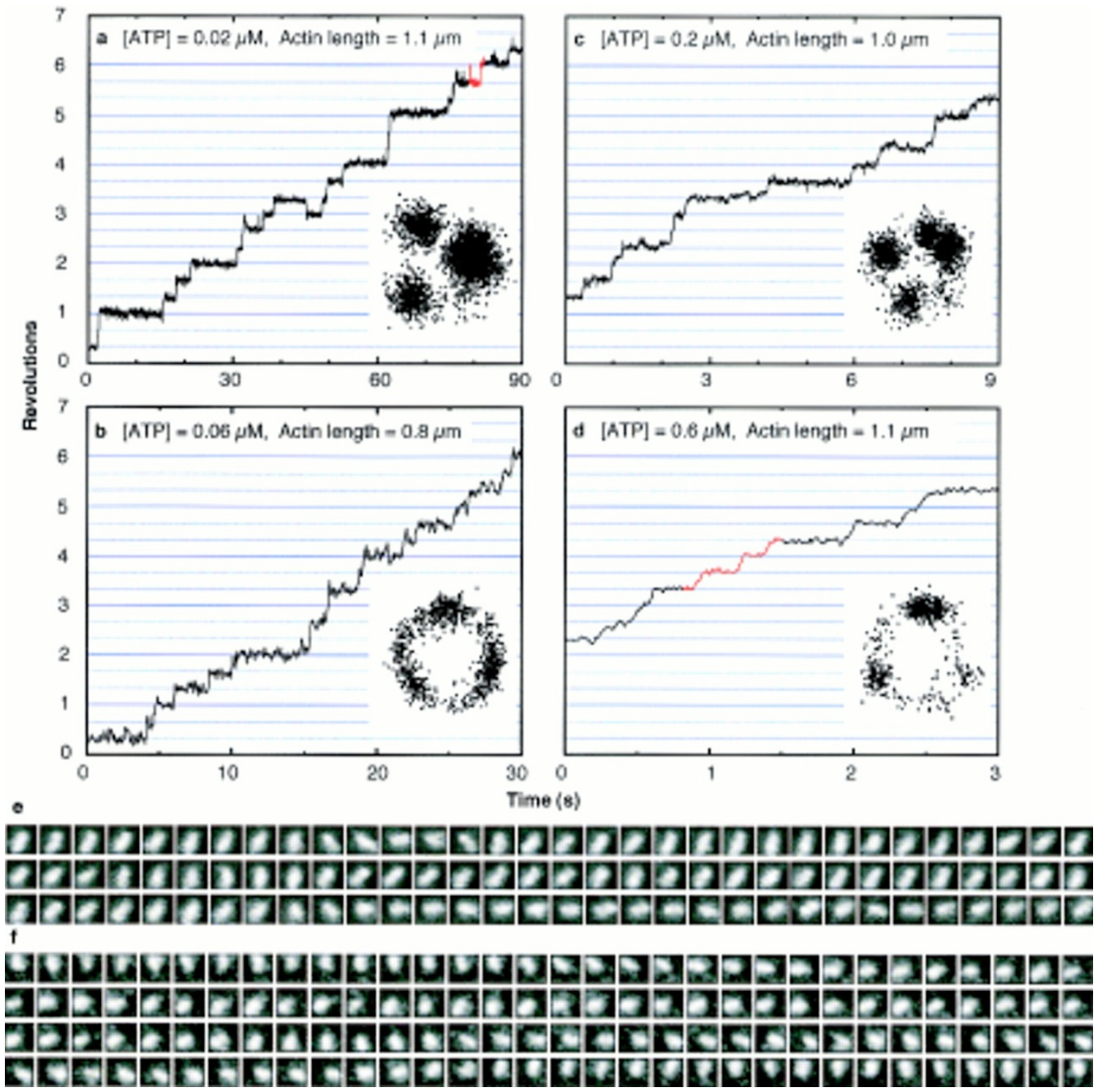
a [ATP] = 0.02 μM, Actin length = 1.1 μm
c [ATP] = 0.2 μM, Actin length = 1.0 μm
b [ATP] = 0.06 μM, Actin length = 0.8 μm
d [ATP] = 0.6 μM, Actin length = 1.1 μm
Revolutions
Time (s)
e
f

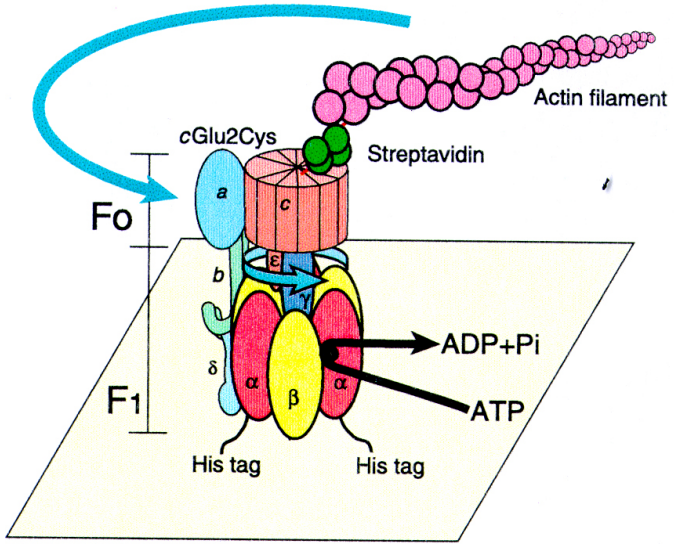

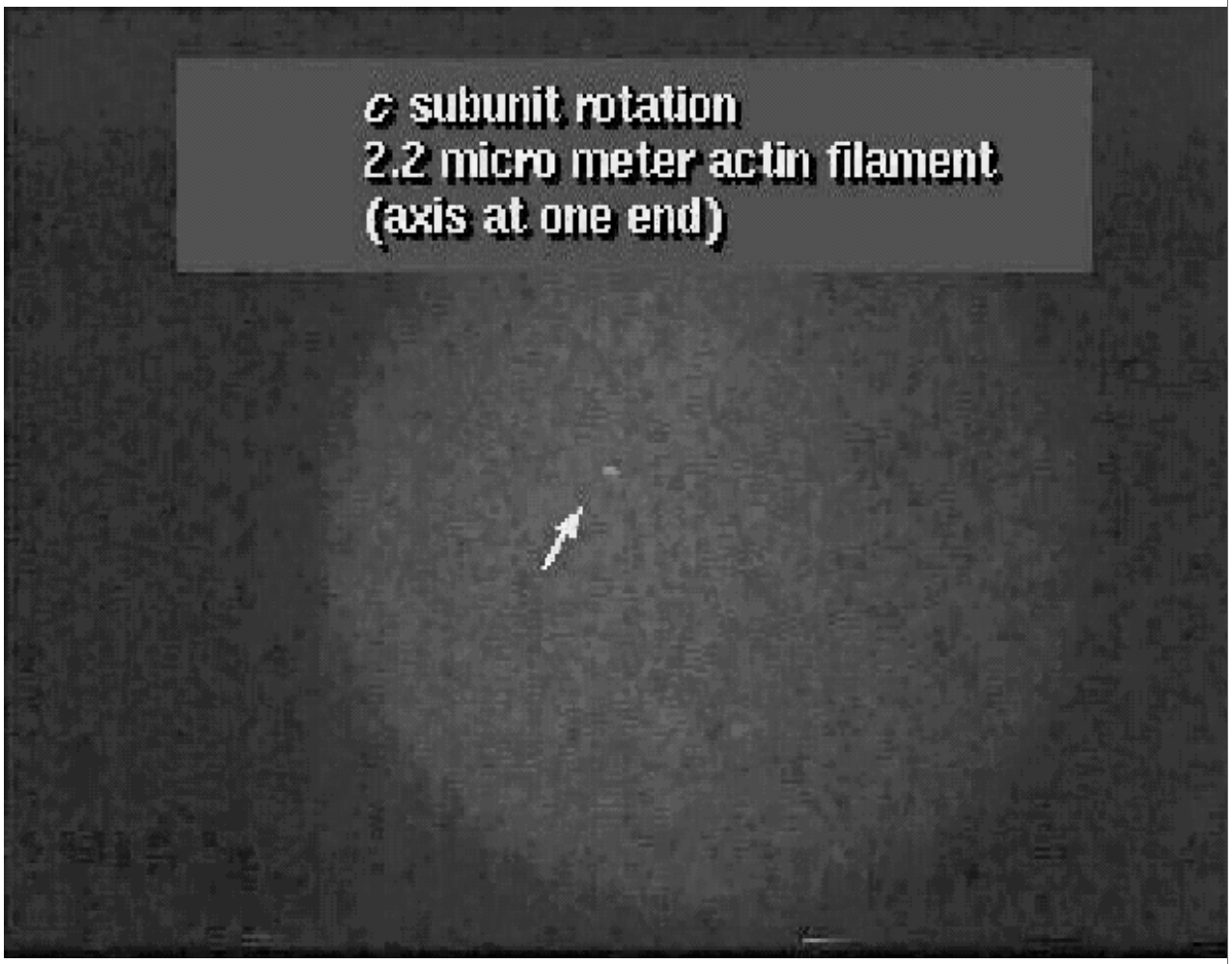

Sambongi *et al. Science* **286**, 1722 - 1724 (1999)

What can rotate ?

Cross-linking Experiments:

Stator-Subunits (α, β, δ, ***a***, ***b***)

Rotor-Subunits (γ, ε, ***c***)

Cross-linking within one group is OK

Cross-linking between two groups inhibits function.

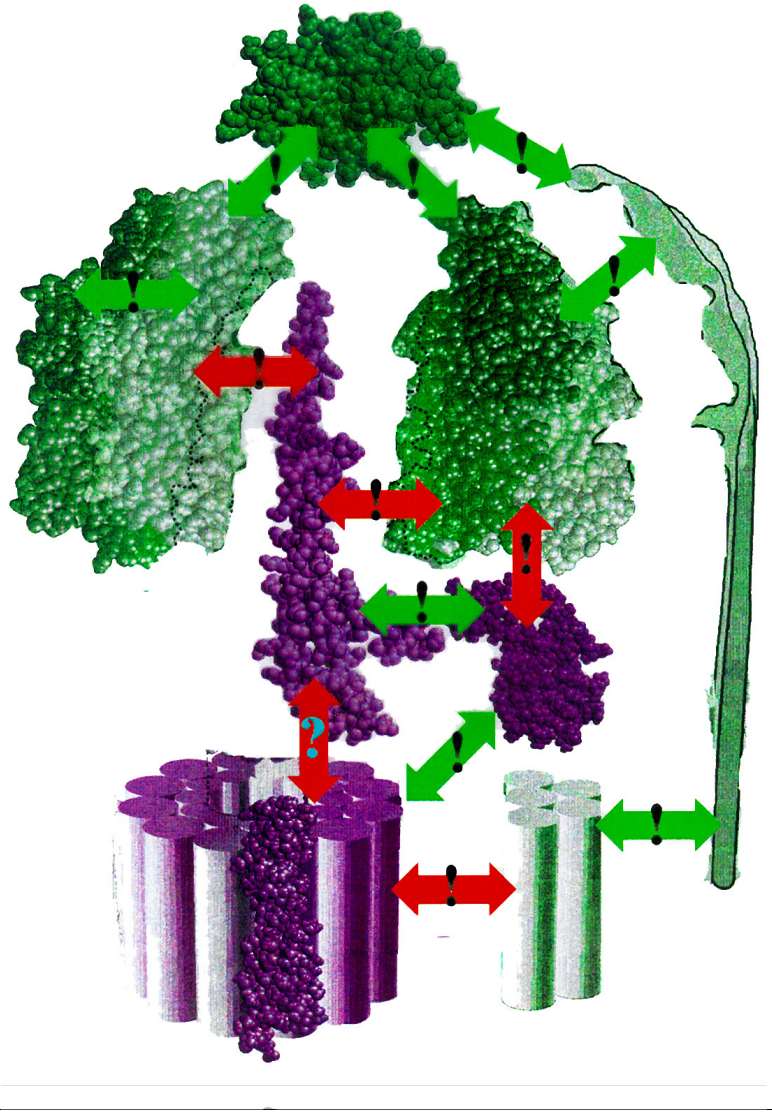

cross-linking γ with α or β (experimental layout)

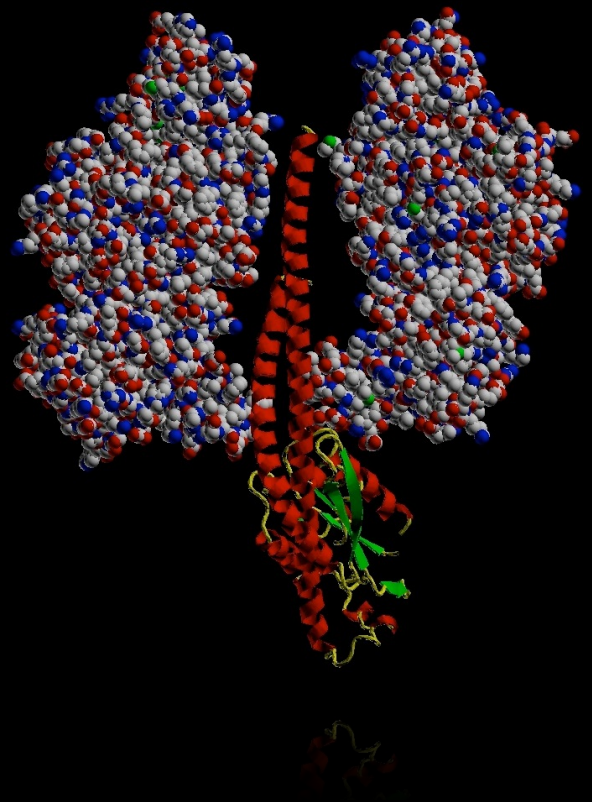

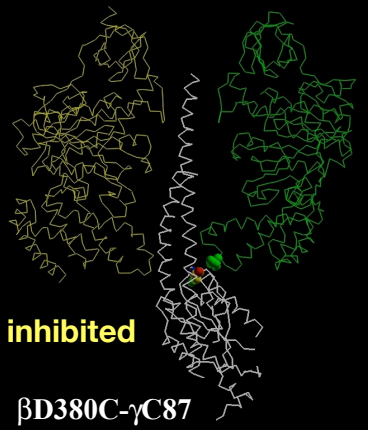

inhibited

βD380C-γC87

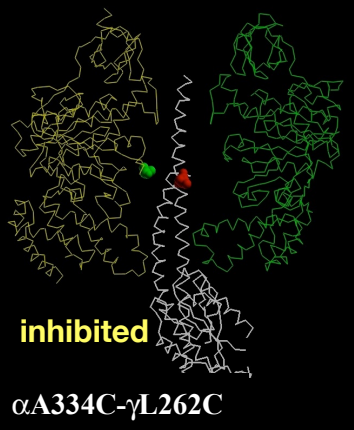

inhibited

αA334C-γL262C

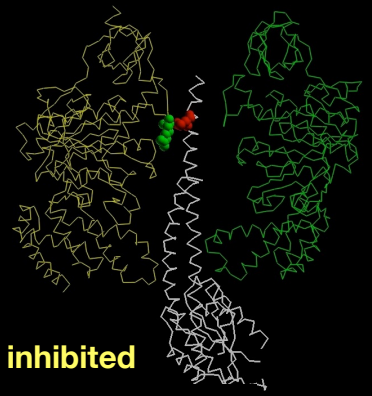

inhibited

αR283C-γL276C

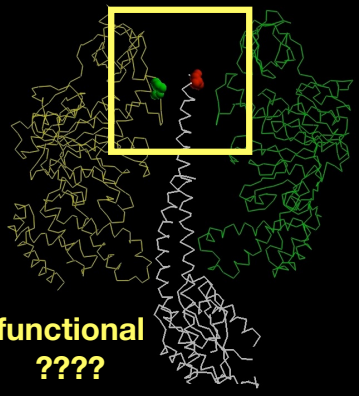

functional
????

αP280C-γA285C

Gumbioski *et al.* (Sigi Engelbercht group), JBC 2001

The torque developed from ATP hydrolysis is sufficient to overcome Ramachandran restrictions

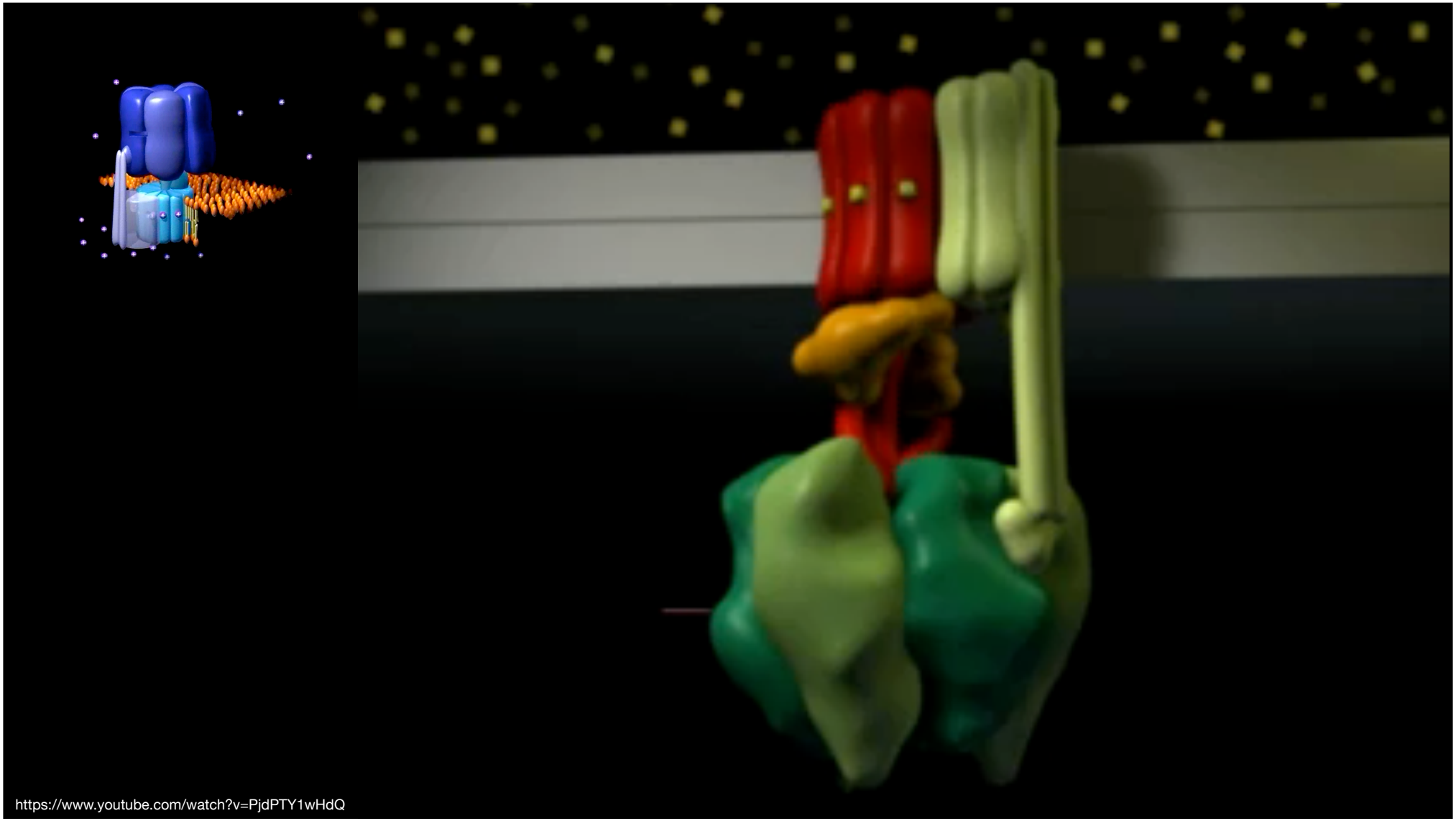
https://www.youtube.com/watch?v=PjdPTY1wHdQ

F-type ATPases

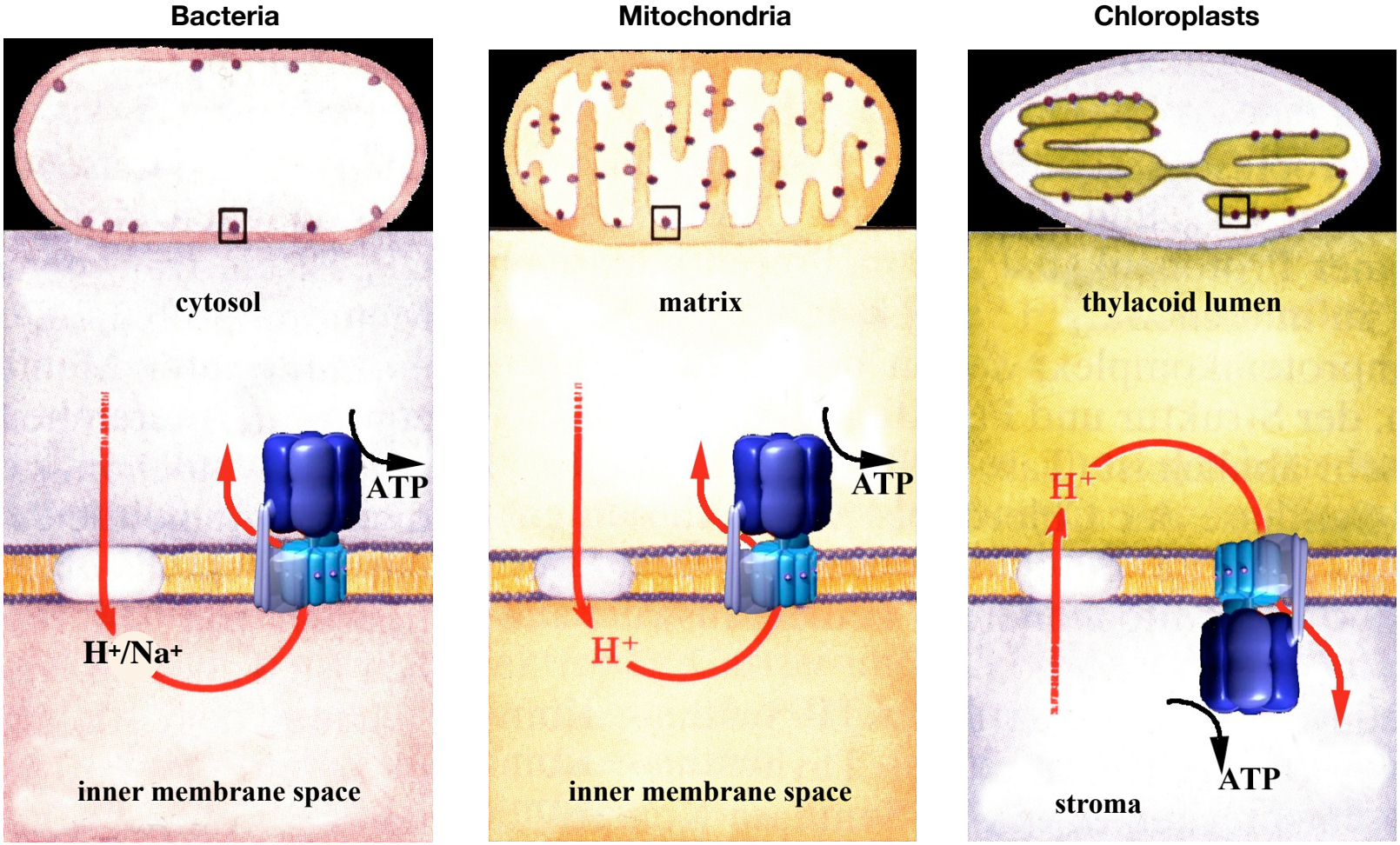

adapted from Lehninger (1994)

Structure Determination of yeast F1c10 ATP synthase

Amplitudes: Dataset to 3.9 Å from beamline ID2, Grenoble.

Crystal: Spacegroup P21, a=136Å, b=178Å, c=139Å, β= 91.5º, 1 Molecule/AS.

Phases: Molecular replacement with bovine F1 ATPase Cα coordinates as search model.

Refinement: Solvent flattening (~ 60% solvent content).

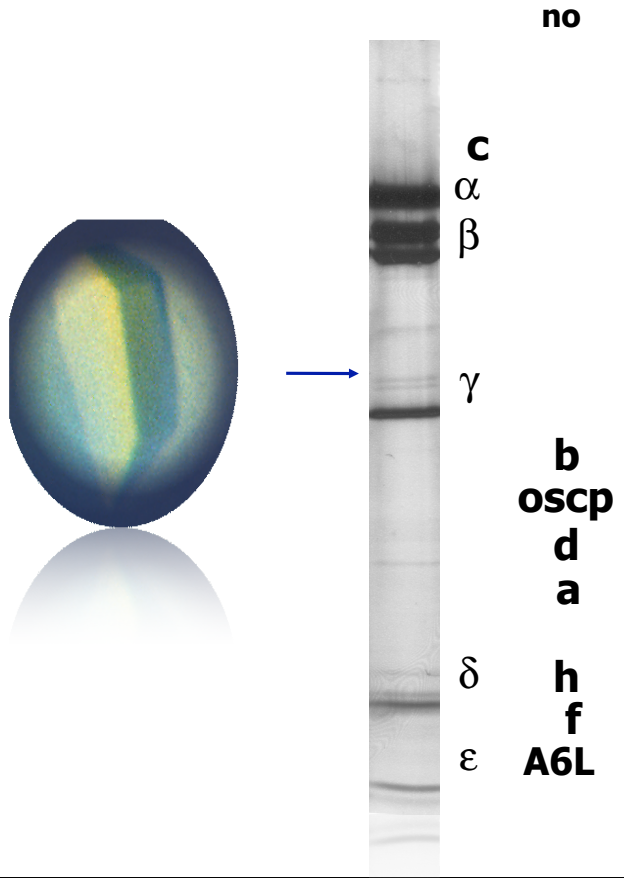

Stock *et al.*, Science (1999)

The ATP Synthase from Yeast Mitochondria

X-Ray Diffraction

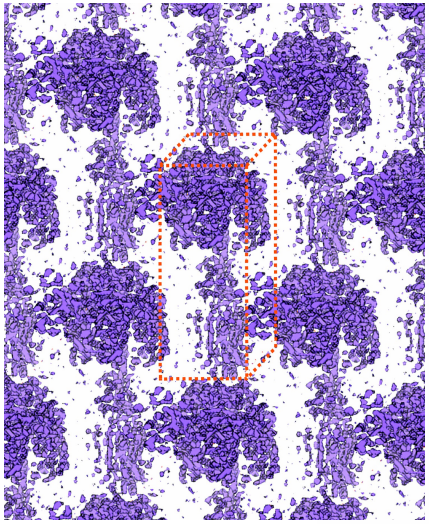

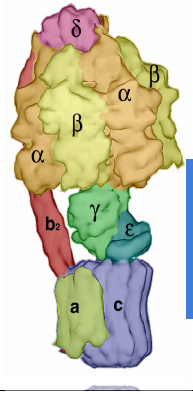

The subunits a, b and δ were missing.

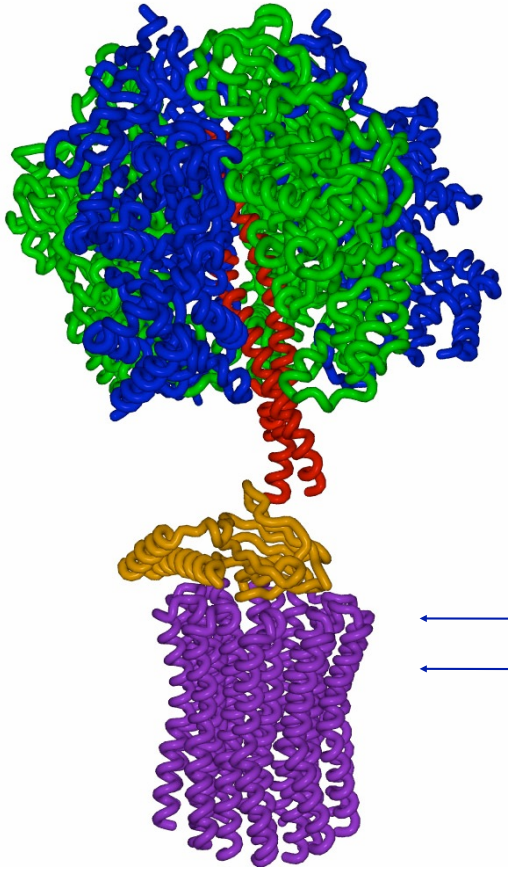

3.9 Å resolution

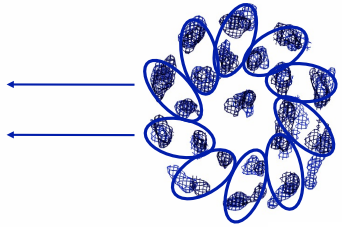

10 subunits *c*

Stock *et al.*, Science (1999)

A model for the ATP Synthase

Locations of the a, b_2, and δ subunits are speculation.

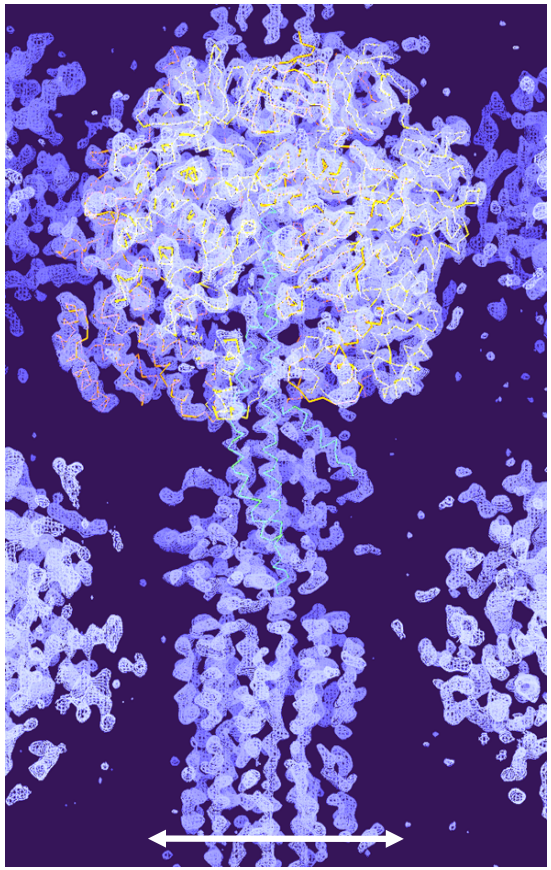

0,000 000 008 m

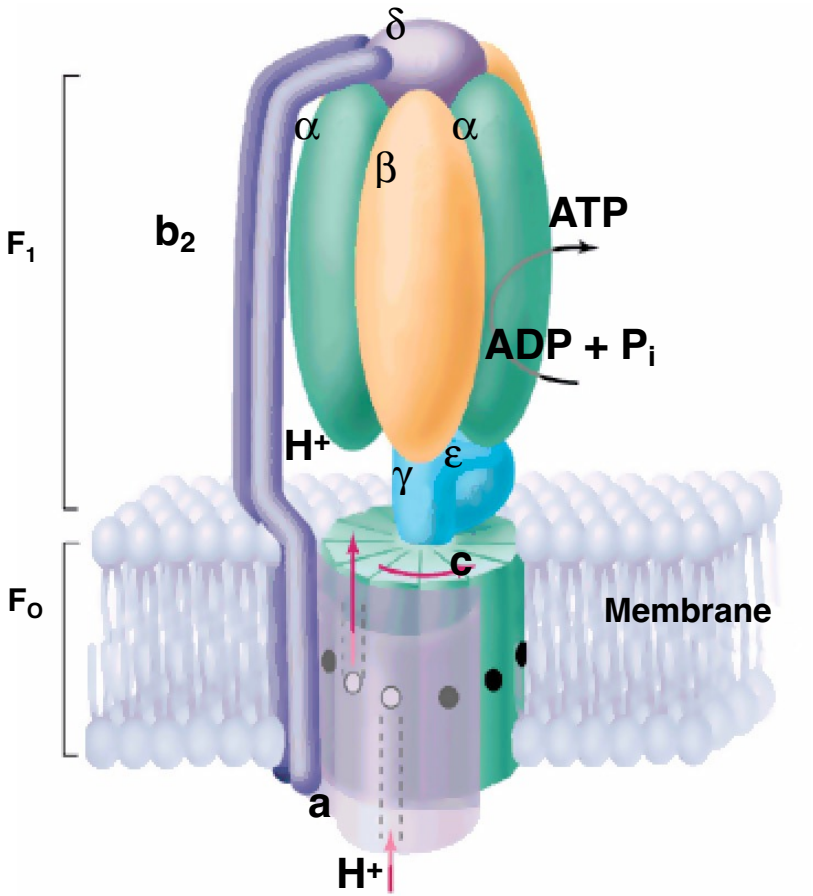

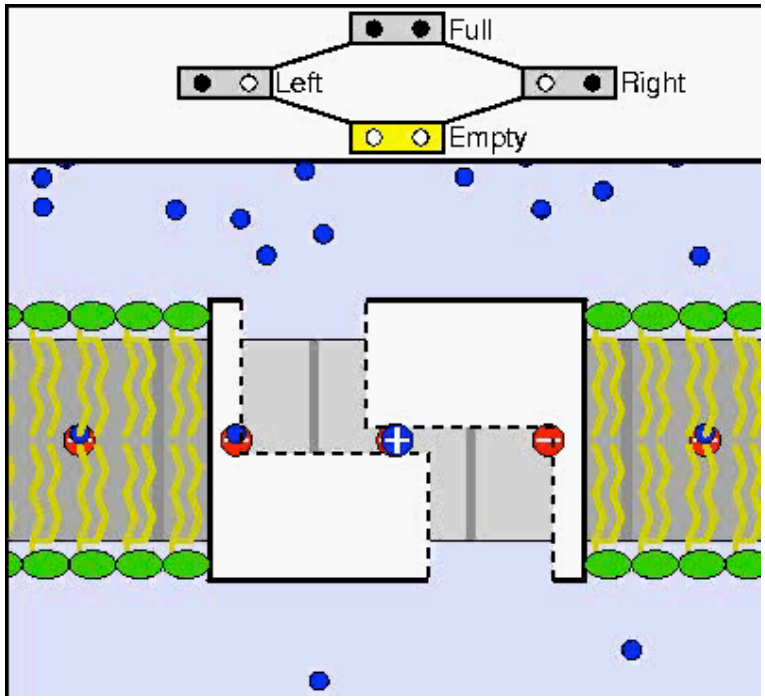

1000 rpm with 8 nm diameter gives a rotation speed of 2.5 μm/s

No Friction !

Ratchet Motor !

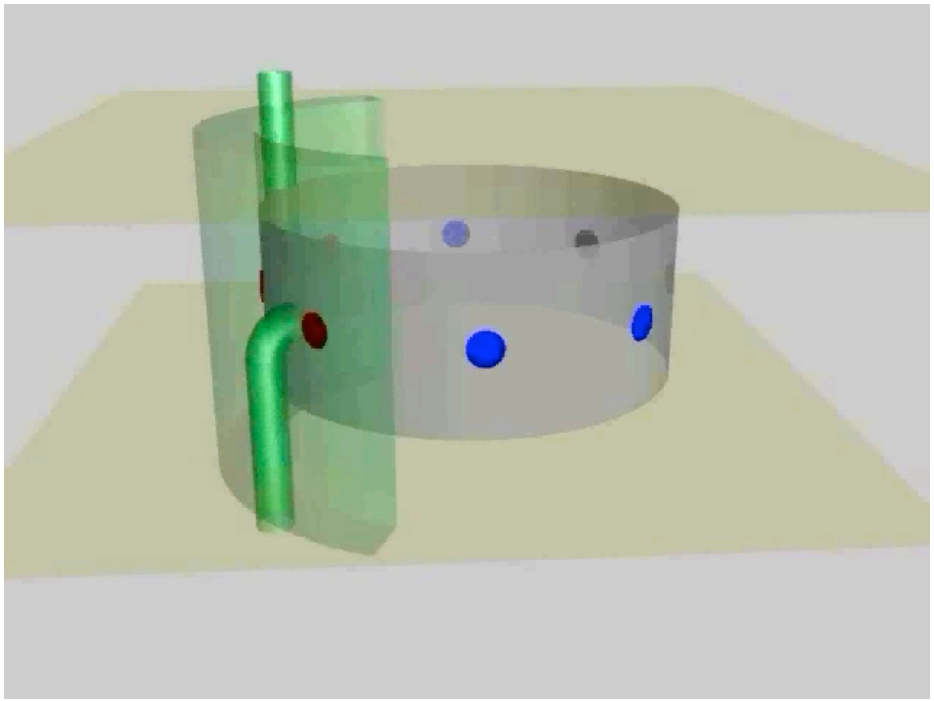

Brownian Motion at 300K for a proton:

$E = kT = 1/2 * m * v^2$

=> $v = \sqrt{2 * k * T / m}$

k = Boltzmann constant = $1.38*10^{-23}$ $m^2kg^2s^{-2}K^{-1}$

T = Temperature = 300K

m = mass of a proton = $1.67*10^{-27}$ kg

$v = \sqrt{2 * 1.38*10^{-23} * 300 / 1.67*10^{-27}}$

= 2226 m/s

Ratchet Motor,
driven by Brownian motion

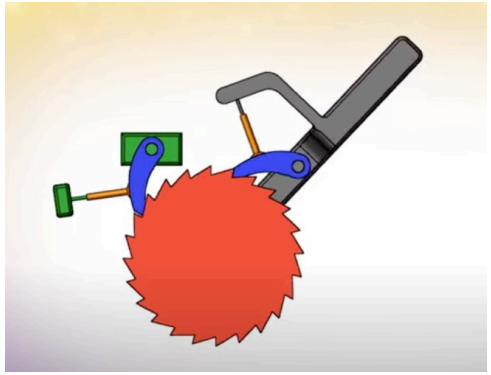

https://youtu.be/EpVPG2fZrHE

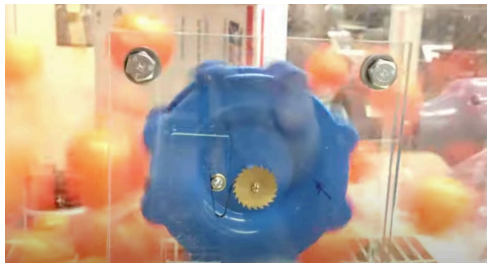

https://youtu.be/QU2CKQQLDt4

Efficiency

How much energy does the Proton Motive Force give for protons that traverse the membrane?

PMF := 2.3 RT ΔpH + F ΔΨ

R = Gas Constant = 8.315 J/mol/K
T = Temperature (= 300 Kelvins at room temperature)
F = Faraday Constant = 96.5 kJ/V/mol
ΔΨ = electrical membrane potential = 200 mV

How much energy does the hydrolysis of ATP give?

ATP-Energy = ΔG(ATP → ADP+P_i)

$$\Delta G = \Delta G^0 + RT \ln \frac{[\mathrm{ADP}][\mathrm{P_i}]}{[\mathrm{ATP}]}$$

Typically: [ADP]=0.25 mM, [P_i]=2.0 mM, [ATP]=2.5 mM

$$\Delta G = \Delta G^0 + RT \ln\left(\frac{0.25 \cdot 10^{-3} \cdot 2.0 \cdot 10^{-3}}{2.5 \cdot 10^{-3}}\right)$$

$$\Delta G = \Delta G^0 + RT \ln(0.0002)$$

Therefore:
ΔG = -30.5 kJ/mol - 21.2 kJ/mol = -51.7 kJ/mol

Efficiency

ITAIPU

Waterflow ∗ Waterpressure

↓

Current ∗ Tension

Waterflow in 18 turbines = 12‘600 m^3/s
Waterforce = 118m*g = 1158 N
g = gravity constant = 9.81 N/m (on Earth)
Waterpower = 12‘600‘000 liter/s * 1158 N
= 14‘591‘000 Watt = 14.6 GigaWatt
ITAIPU Nominal Output = 14 GigaWatt
ITAIPU Average Output 2016 = 11.7 GigaWatt
Efficiency = ~80%

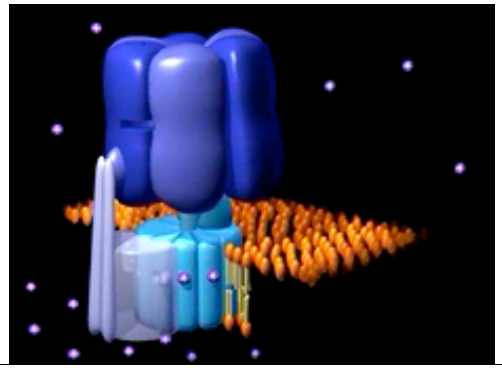

ATP Synthase

Proton-flow ∗ Proton-Motive Force (PMF)

↓

ATP-Flow ∗ ATP-Energy

$PMF := RT \ln([H^+]^i / [H^+]^o) + F \Delta\Psi$
$= \log(e)\, RT\, \Delta pH + F\, \Delta\Psi$
$= 2.3\, RT\, \Delta pH + F\, \Delta\Psi$

R = Gas Constant = 8.315 J/mol/K
T = Temperature (= 300 Kelvins)
F = Faraday Constant = 96.5 kJ/V/mol
$\Delta\Psi$ = electrical membrane potential

Assuming $\Delta pH = 0.7$, $\Delta\Psi = 70mV$; then: PMF = 10.7 kJ/mol
Input = 14 protons cross the membrane = 14 * PMF
$= 14 * (2.3\, RT\, \Delta pH + F\, \Delta\Psi)$
= 14 * (2.3 * 8.315J/mol/K * 300K * 0.7 + 96.5 kJ/V/mol * 0.070V)
= 14 * 10.7 kJ/mol = 150 kJ/mol

ATP-Energy = $\Delta G(ATP \rightarrow ADP + P_i)$ = -50 kJ/mol
Output = 3 ATP synthesized = 3 * 50 kJ/mol = 150 kJ/mol
Efficiency (3 ATP for 14 protons) = 100 %

Typical for Chloroplasts: in Thylokoid: pH=5; in Stroma: pH=7.8
With a membrane potential of 200mV, how much is 14*PMF?

F-ATPases

I. tartaricus **(Bacteria)**

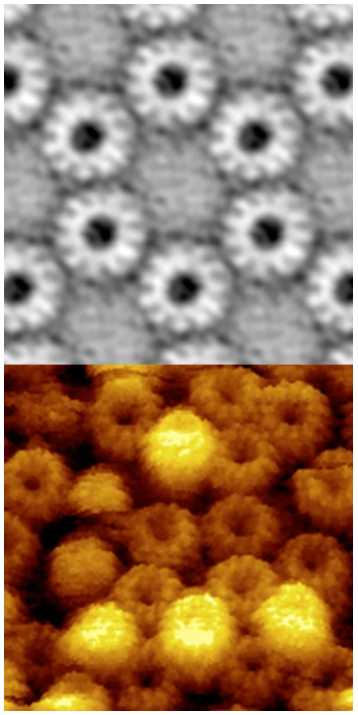

I. tartaricus**:**
11 Na^+ / 3 ATP

Mitochondria

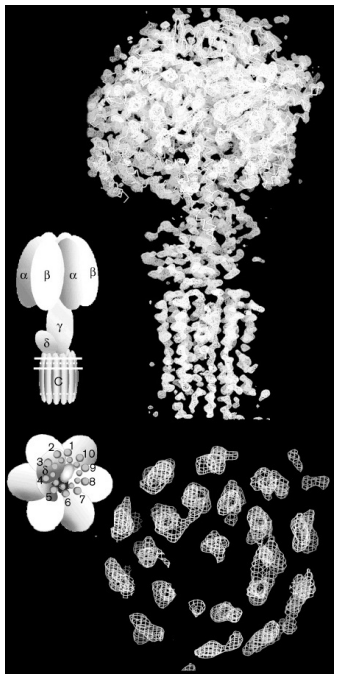

yeast:
10 H^+ / 3 ATP
(+ 3 H^+ / 3 ATP)

Chloroplasts

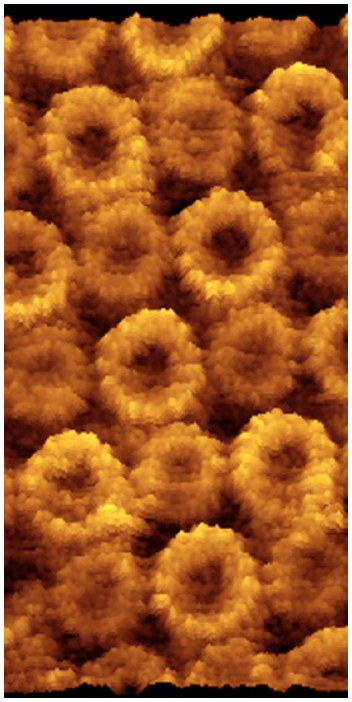

spinach:
14 H^+ / 3 ATP

S. platensis **(Bacteria)**

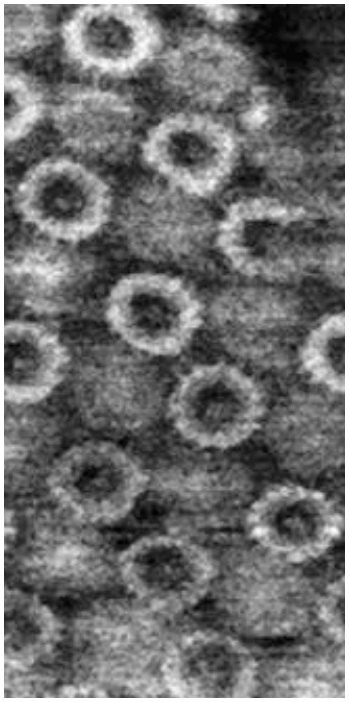

S. platensis**:**
15 H^+ / 3 ATP

F-type ATPases

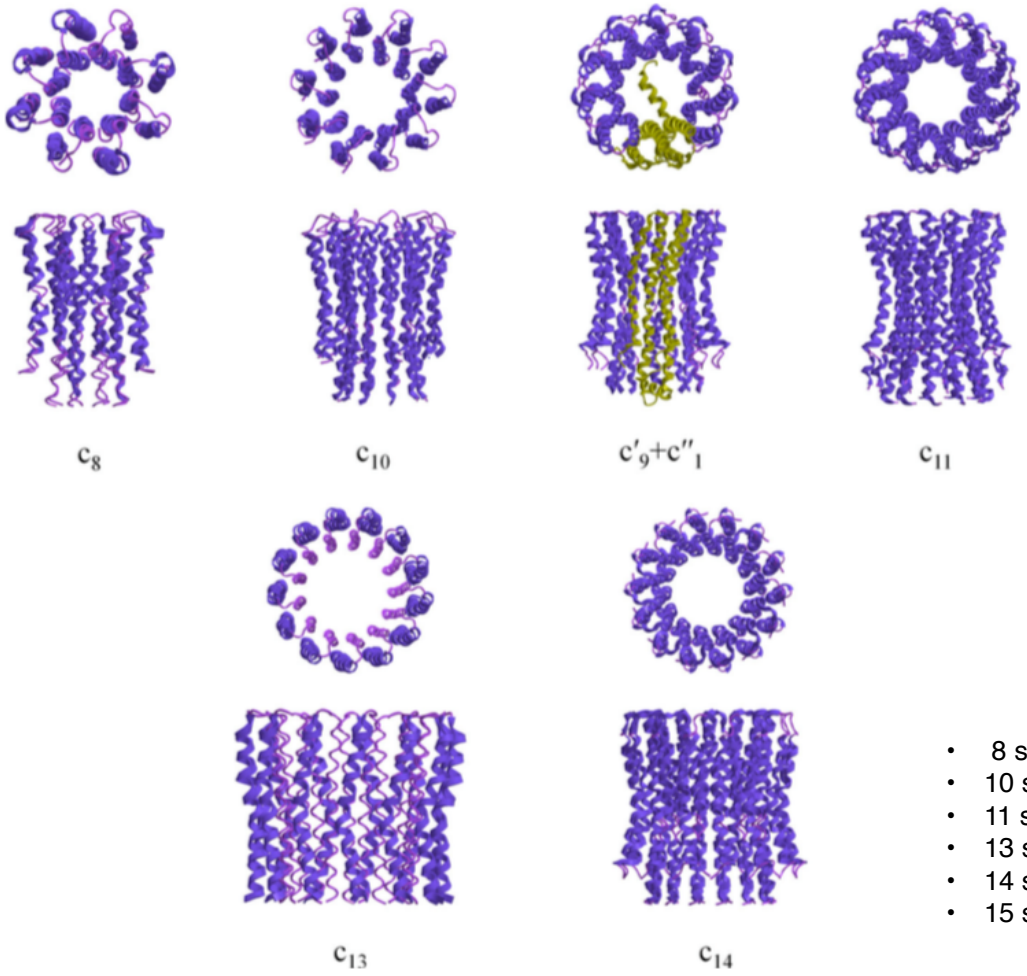

- 8 subunits for bos taurus (PNAS **107** (2010) 16823)
- 10 subunits for yeast (Science **286** (1999) 1700)
- 11 subunits for bacteria *I.tartaricus* (EMBO Rep. **2**(3) (2001) 229)
- 13 subunits for bacteria *B. pseudofirmis* (PNAS **110** (2013) 7874)
- 14 subunits for spinach chloroplast (Nature **405** (1999) 418)
- 15 subunits for bacteria *S. platensis* (EMBO Rep. 6(11) (2005) 1040)

The cation powered rotor of ATP synthase

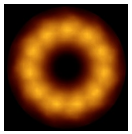

Rotor stoichiometry varies between organisms:

10 subunits for yeast (Science **286** (1999) 1700)
14 subunits for spinach chloroplast (Nature **405** (1999) 418)
11 subunits for bacteria *I.tartaricus* (EMBO Rep. **2**(3) (2001) 229)
15 subunits for bacteria *S. platensis* (EMBO Rep. **6**(11) (2005) 1040)

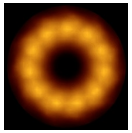

Rotor stoichiometry does not vary within one organism.
The cation-to-ATP ratio of ATP synthesis should therefore be constant within one organism.

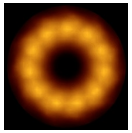

Rotor diameter appears to be defined by its transmembrane subunits.

LETTER

214 | NATURE | VOL 481 | 12 JANUARY 2012

doi:10.1038/nature10699

Subnanometre-resolution structure of the intact *Thermus thermophilus* H^+-driven ATP synthase

Wilson C. Y. Lau[1,2] & John L. Rubinstein[1,2,3]

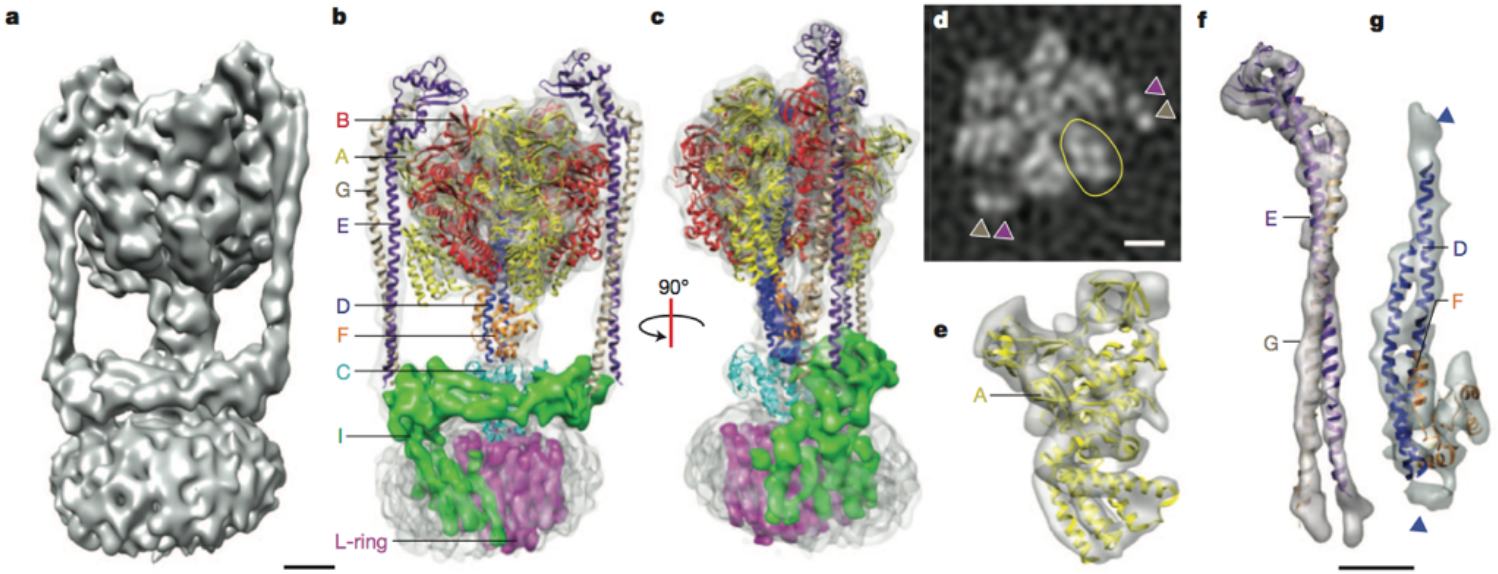

Figure 1 | Three-dimensional map of the *T. thermophilus* ATP synthase. **a**, A surface view of the three-dimensional map. **b**, **c**, The overall map (semi-transparent grey) with fitted crystal structures and segments corresponding to individual subunits. Segments of the cryo-EM map are shown for the L_{12} ring, subunit I and residues of subunit D missing from its crystal structure. **d**, A cross-section through the soluble region of the map shows that α-helices from the two E subunits (purple arrows) and two G subunits (beige arrows) can be resolved. Helices can also be resolved in other subunits, such as the A subunits (example circled in yellow). The map segments agree with crystal structures, such as subunit A (**e**), the EG subcomplex (**f**) and the DF subcomplex (**g**). Density corresponding to missing residues from the crystal structure of the D subunit is indicated with blue arrows. Scale bars, 25 Å.

LETTER

214 | NATURE | VOL 481 | 12 JANUARY 2012

doi:10.1038/nature10699

Subnanometre-resolution structure of the intact *Thermus thermophilus* H^+-driven ATP synthase

Wilson C. Y. Lau[1,2] & John L. Rubinstein[1,2,3]

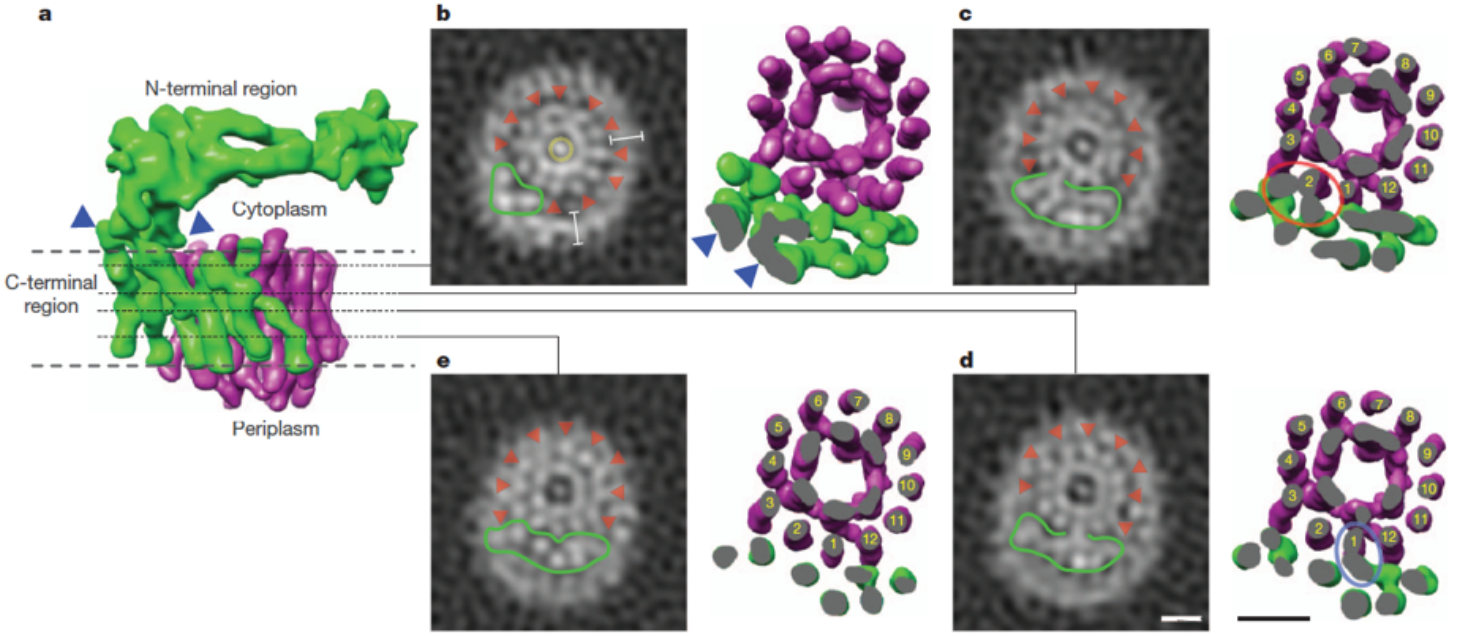

Figure 3 | The membrane-bound region of the enzyme. **a**, Map segments of the L_{12} ring (magenta) and subunit I (green) showing multiple contacts between the N- and C-terminal regions of subunit I (blue arrows). **b**, Cross-sections through the map (left panel) and map segments truncated at the same height (right panel) show subunit I separated from the L_{12} ring near the cytoplasm. Outer helices of the L_{12} ring are indicated (red arrows) and the transmembrane helices of subunit I are outlined (green). Cross-sections show the detergent micelle (white bars) and detergent or lipid in the centre of the L_{12} ring (yellow circle). **c**, Near the middle of the membrane, subunit I contacts an L subunit, probably forming the mid-membrane end of the cytoplasmic half channel (circle in red in right panel). **d**, Approximately 6 Å further towards the periplasm subunit I contacts a different L subunit, probably forming the mid-membrane end of the periplasmic half-channel (circled in blue in right panel). **e**, Subunit I is separated from the L_{12} ring near the periplasm. Scale bars, 25 Å.

NATURE | LETTER

日本語要約

Horizontal membrane-intrinsic α-helices in the stator *a*-subunit of an F-type ATP synthase

Matteo Allegretti, Niklas Klusch, Deryck J. Mills, Janet Vonck, Werner Kühlbrandt & Karen M. Davies

Affiliations | Contributions | Corresponding authors

Nature **521**, 237–240 (14 May 2015) | doi:10.1038/nature14185
Received 28 August 2014 | Accepted 29 December 2014 | Published online 23 February 2015

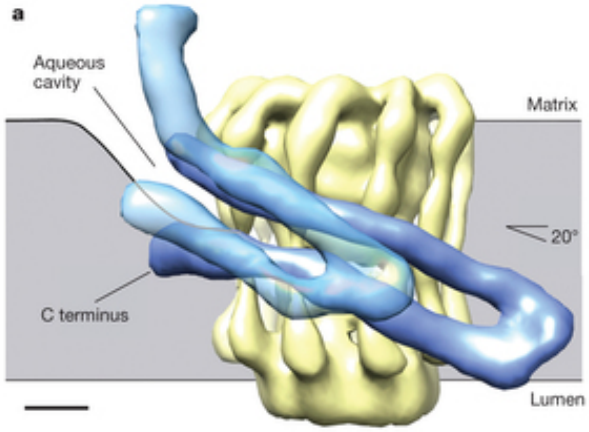

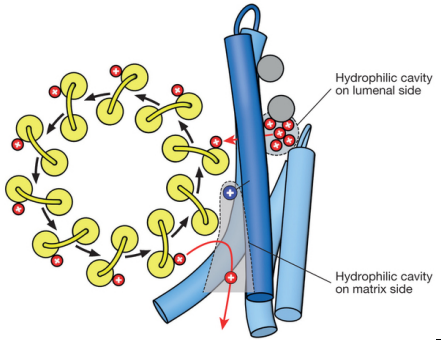

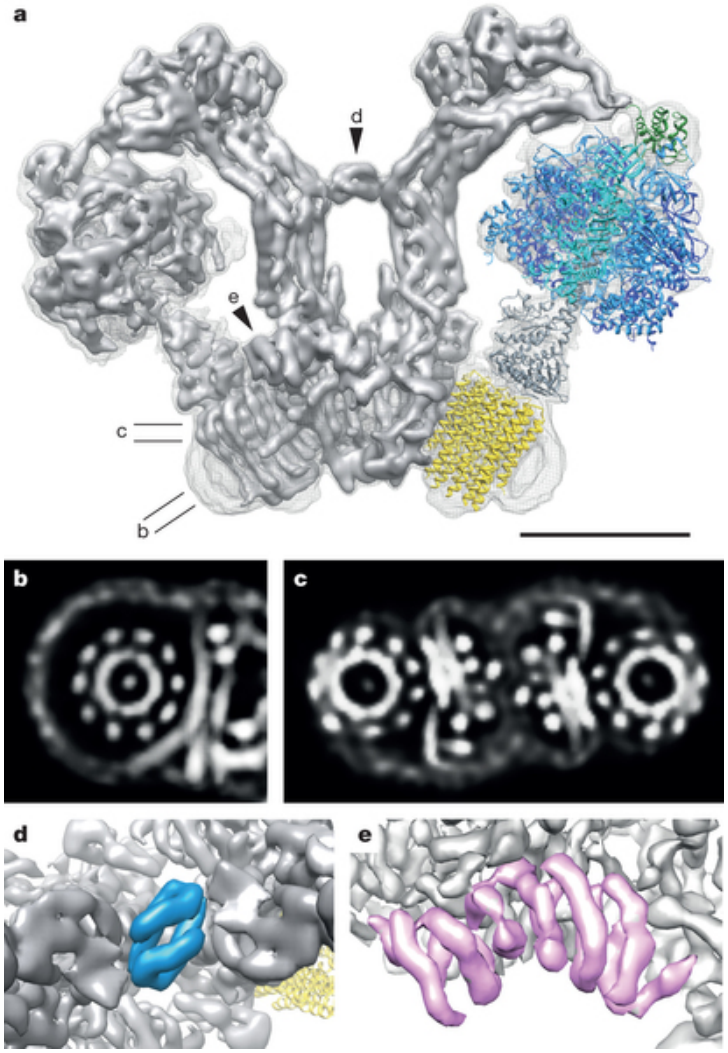

Structure and conformational states of the bovine mitochondrial ATP synthase by cryo-EM

Anna Zhou, Alexis Rohou, Daniel G Schep, John V Bason, Martin G Montgomery, John E Walker ✉, Nikolaus Grigorieff ✉, John L Rubinstein ✉

The Hospital for Sick Children Research Institute, Canada; The University of Toronto, Canada; Janelia Research Campus, Howard Hughes Medical Institute, United States; MRC Mitochondrial Biology Unit, United Kingdom

DOI: http://dx.doi.org/10.7554/eLife.10180
Published October 6, 2015
Cite as eLife 2015;4:e10180

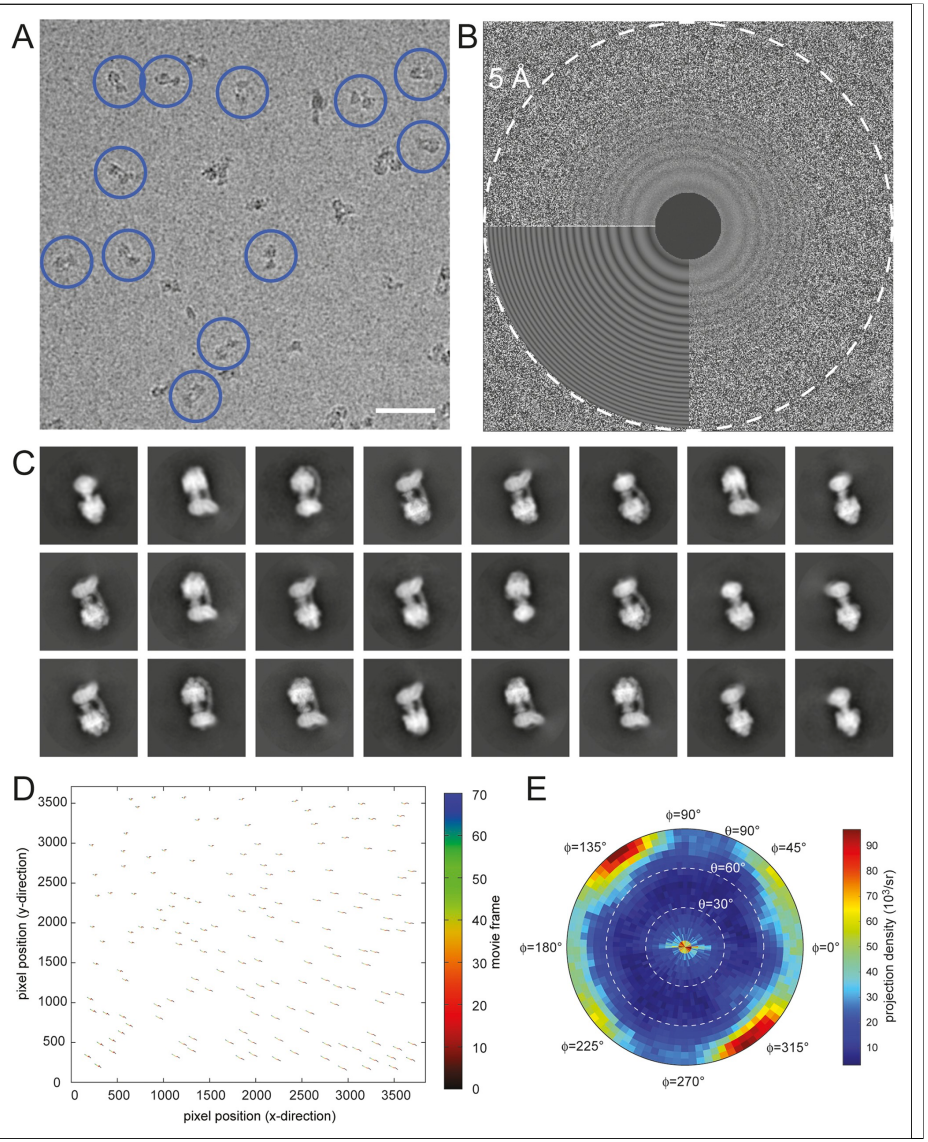

Structure and conformational states of the bovine mitochondrial ATP synthase by cryo-EM

Anna Zhou, Alexis Rohou, Daniel G Schep, John V Bason, Martin G Montgomery, John E Walker, Nikolaus Grigorieff, John L Rubinstein

The Hospital for Sick Children Research Institute, Canada; The University of Toronto, Canada; Janelia Research Campus, Howard Hughes Medical Institute, United States; MRC Mitochondrial Biology Unit, United Kingdom

DOI: http://dx.doi.org/10.7554/eLife.10180
Published October 6, 2015
Cite as eLife 2015;4:e10180

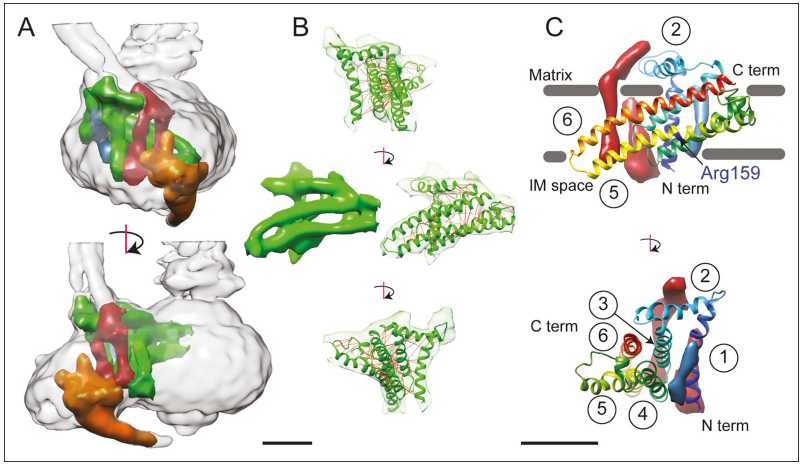

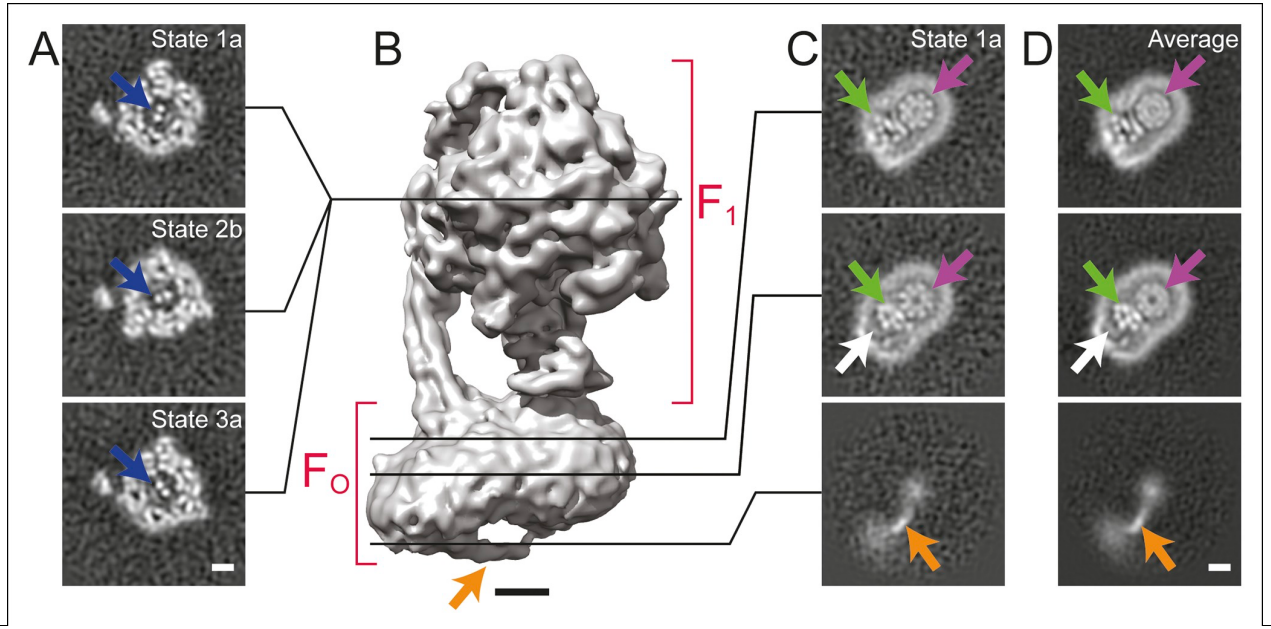

Structure and conformational states of the bovine mitochondrial ATP synthase by cryo-EM

Anna Zhou, Alexis Rohou, Daniel G Schep, John V Bason, Martin G Montgomery, John E Walker, Nikolaus Grigorieff, John L Rubinstein

The Hospital for Sick Children Research Institute, Canada; The University of Toronto, Canada; Janelia Research Campus, Howard Hughes Medical Institute, United States; MRC Mitochondrial Biology Unit, United Kingdom

DOI: http://dx.doi.org/10.7554/eLife.10180
Published October 6, 2015
Cite as eLife 2015;4:e10180

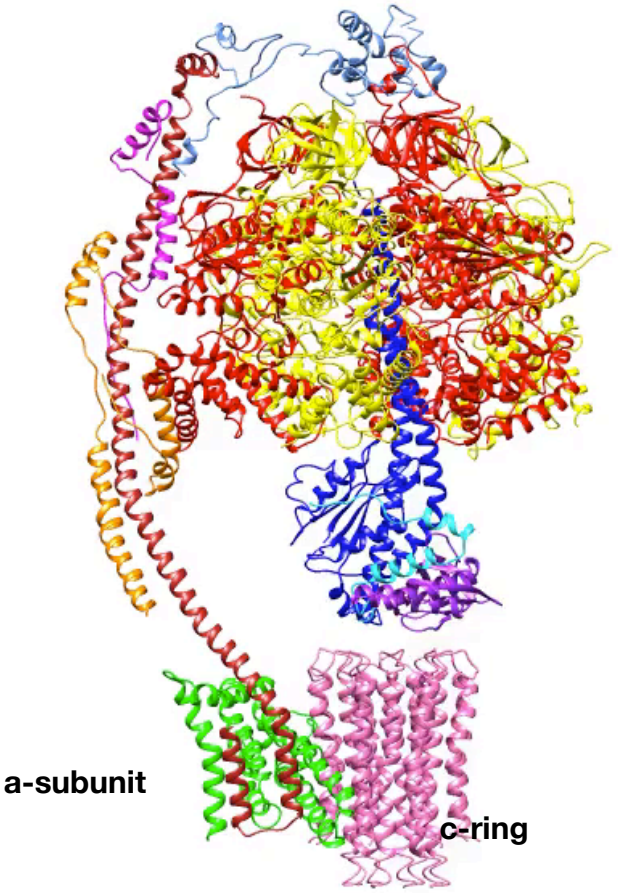

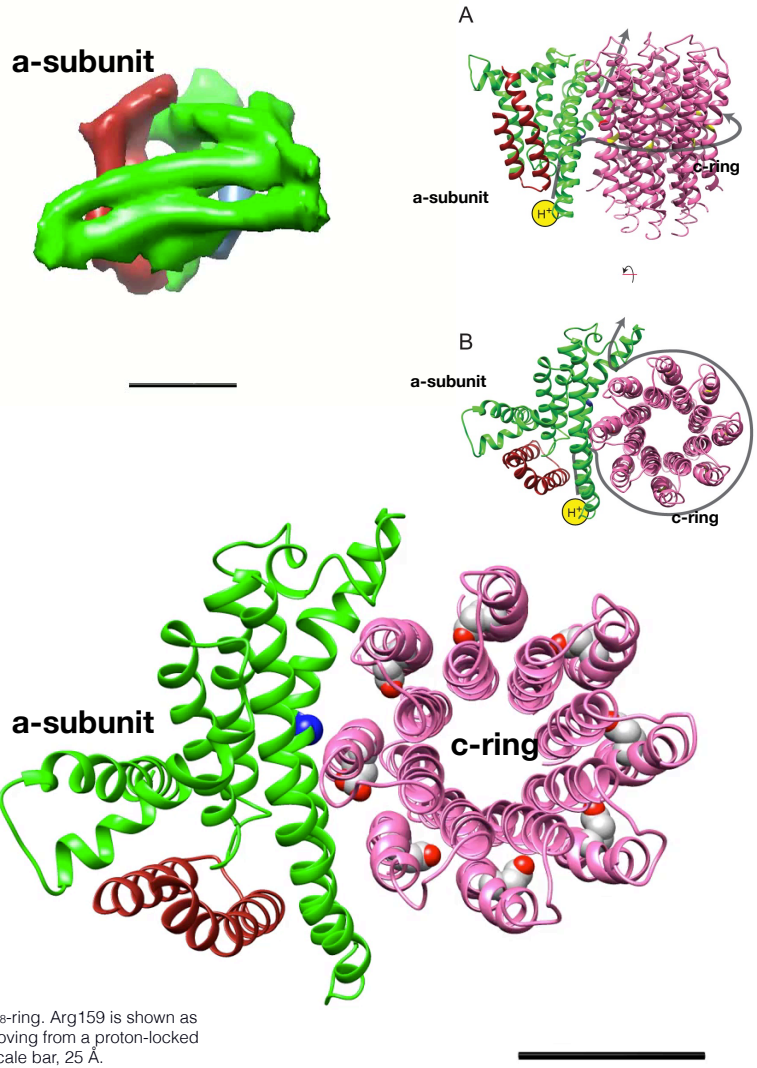

Rotational positions of the c_8-ring. Arg159 is shown as a blue sphere. Glu58 are moving from a proton-locked to an open conformation. Scale bar, 25 Å.

https://elifesciences.org/content/4/e10180

Structure and function of mitochondrial membrane protein complexes

Werner Kühlbrandt

BMC Biology 2015 **13**:89 | **DOI:** 10.1186/s12915-015-0201-x

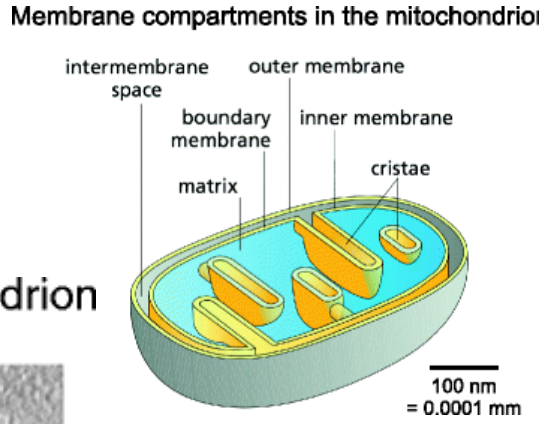

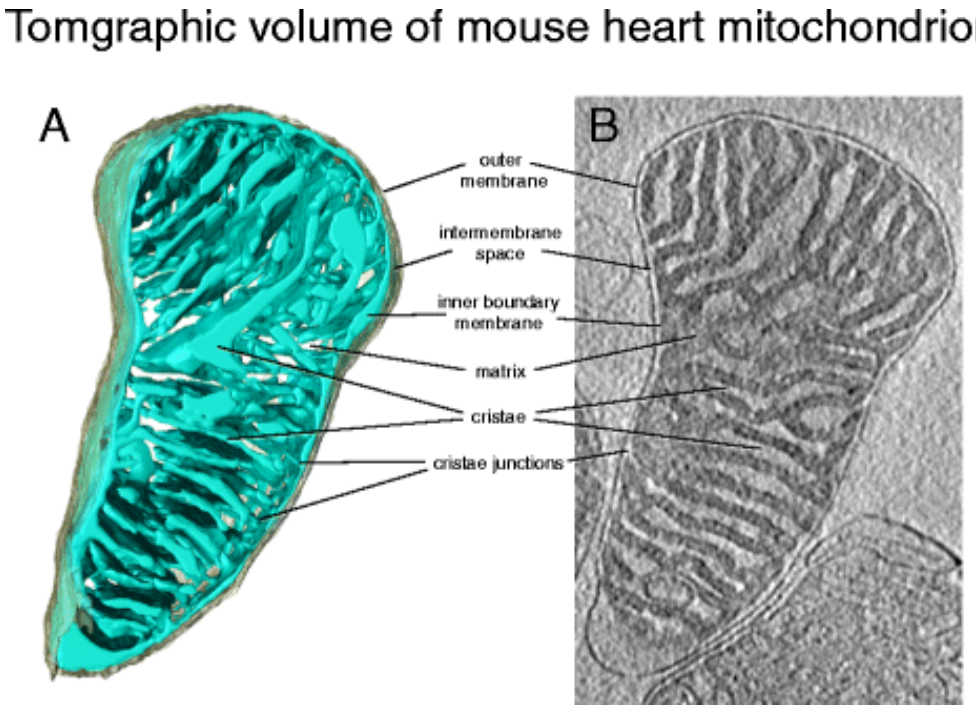

http://www.jove.com/video/51228/visualization-atp-synthase-dimers-mitochondria-electron-cryo

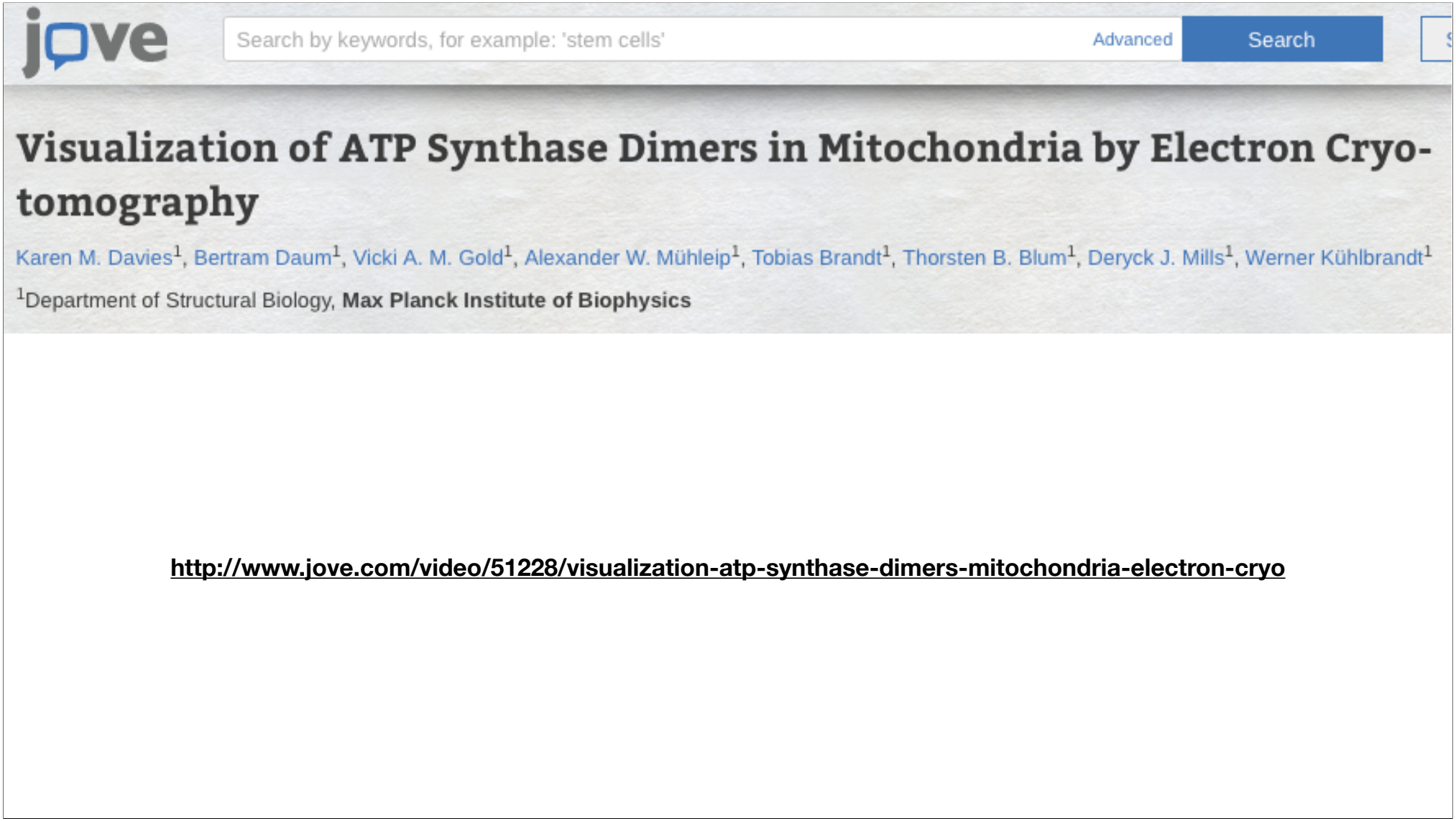
jove
Search by keywords, for example: 'stem cells'
Advanced
Search
Visualization of ATP Synthase Dimers in Mitochondria by Electron Cryo-tomography
Karen M. Davies[1], Bertram Daum[1], Vicki A. M. Gold[1], Alexander W. Mühleip[1], Tobias Brandt[1], Thorsten B. Blum[1], Deryck J. Mills[1], Werner Kühlbrandt[1]
[1]Department of Structural Biology, Max Planck Institute of Biophysics
http://www.jove.com/video/51228/visualization-atp-synthase-dimers-mitochondria-electron-cryo

Structure and function of mitochondrial membrane protein complexes

Werner Kühlbrandt

BMC Biology 2015 **13**:89 | **DOI:** 10.1186/s12915-015-0201-x

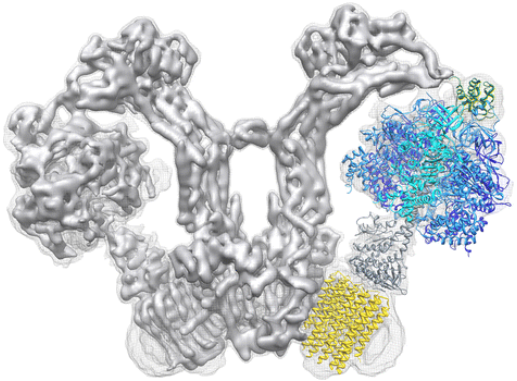

Dimer rows of the mitochondrial ATP synthase in different organisms

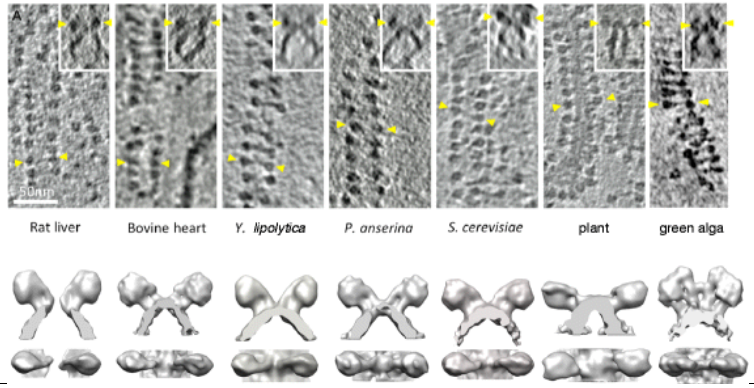

Membrane compartments in the mitochondrion

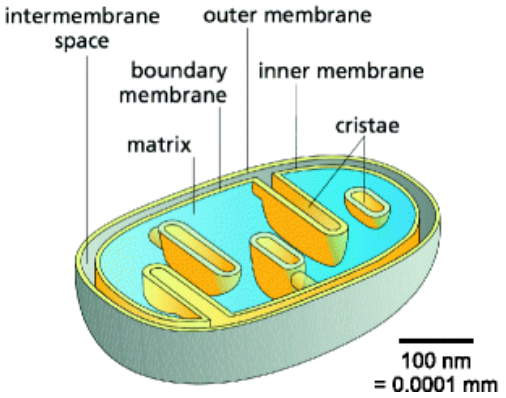

Organisation of mitochondrial cristae

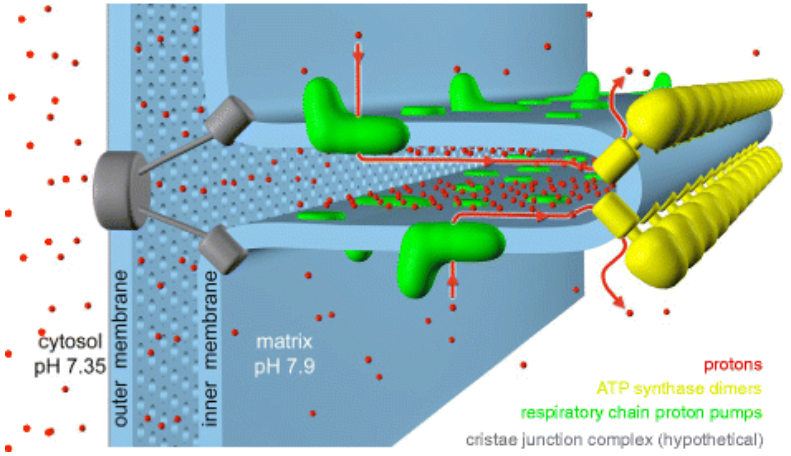

http://www.jove.com/video/51228/visualization-atp-synthase-dimers-mitochondria-electron-cryo

V-ATPases

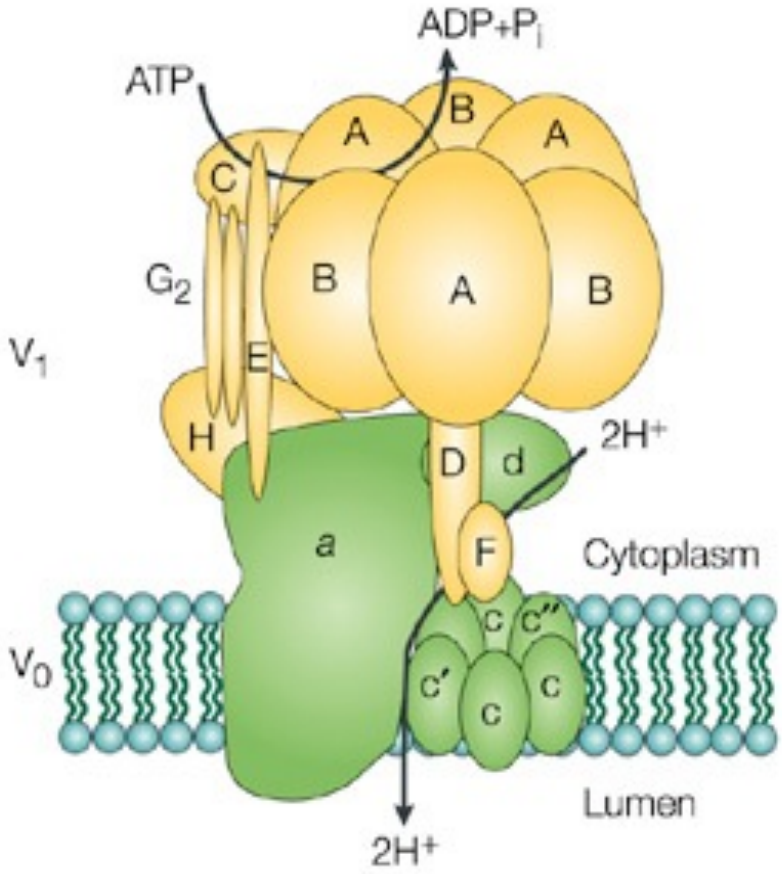

F-ATPases

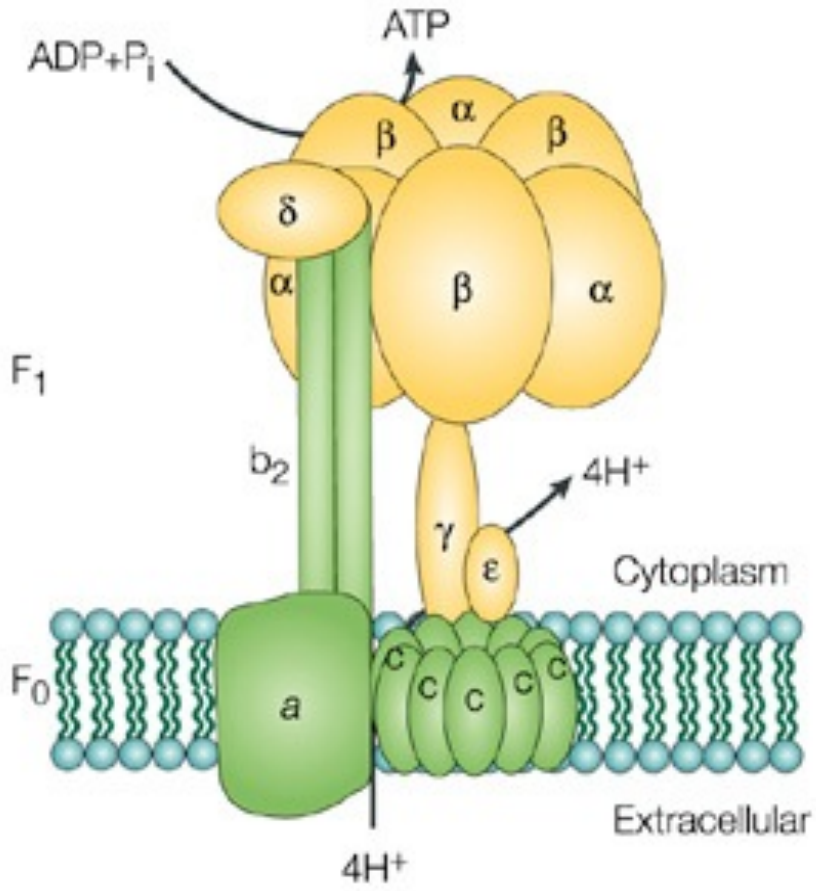

Nature Reviews | Molecular Cell Biology

The V_1 part of the V-ATPase reversibly dissociates

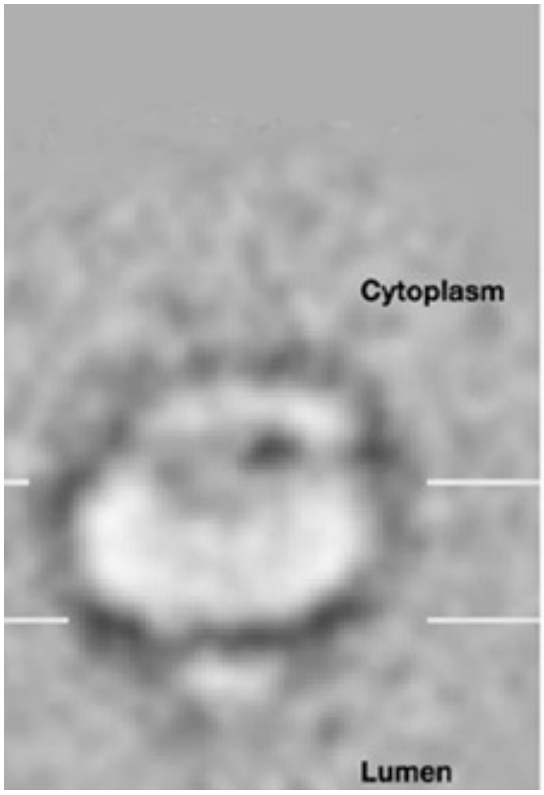

V_O-ATPase

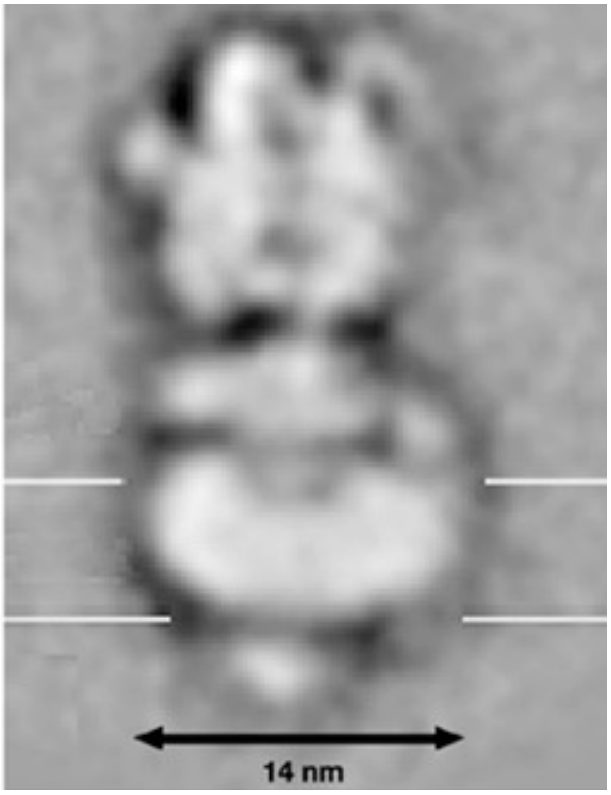

V-ATPase

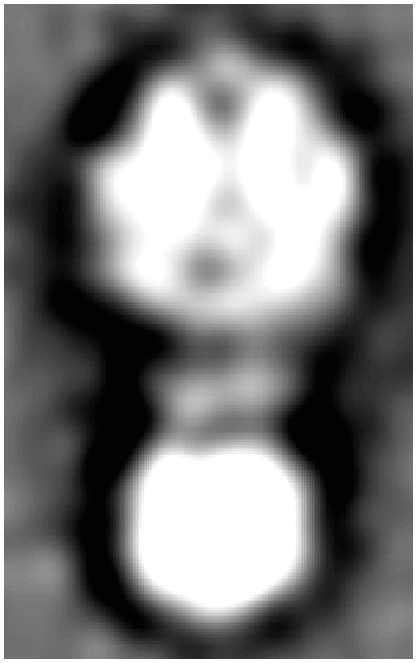

Yeast
F-ATPase

The V-ATPase plays a role in:

- pH regulation in intracellular compartments:
- Endosomes, lysosomes, secretory vesicles.
- bone degradation,
- control of cytoplasmic pH
- Membrane fusion (!?!)
- HIV entry

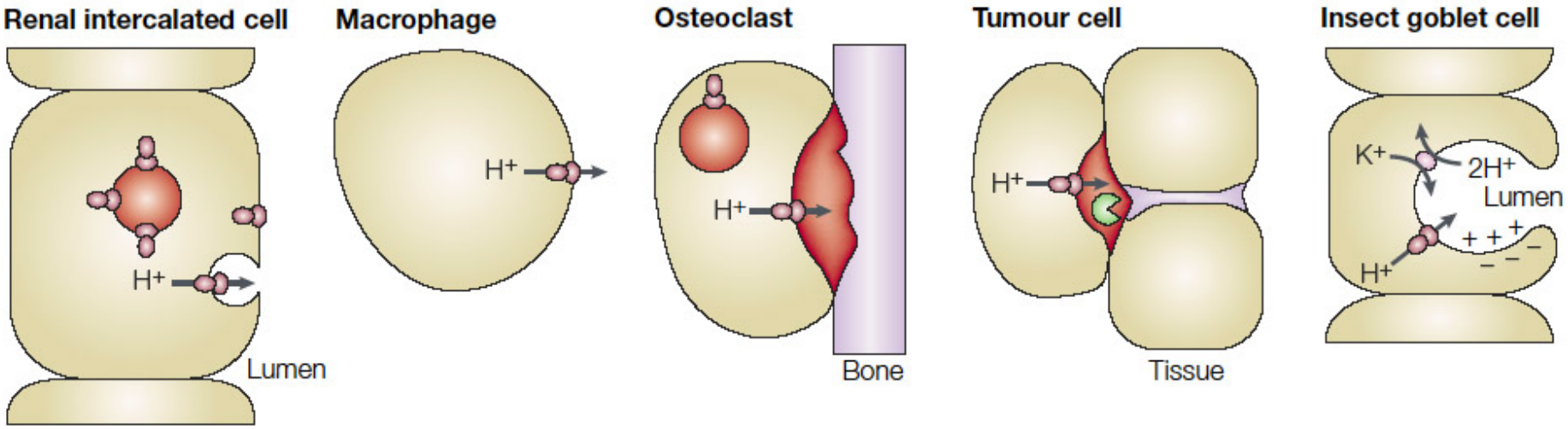

Figure 3 | **Function of plasma membrane V-ATPases.** V-ATPases in renal intercalated cells function in acidification of the urine. Their density in the apical membrane is controlled by reversible fusion of pump-containing intracellular vesicles. V-ATPases in macrophages and neutrophils function in cytoplasmic pH homeostasis. In osteoclasts, V-ATPases are essential for bone resorption, which requires acidification of the space that is in contact with the bone. Tumour cells might use a similar extracellular acidification to promote the activity of secreted lysosomal enzymes that function in metastasis. In insect goblet cells, the V-ATPase creates a lumenal positive membrane potential that drives K^+ secretion through an electrogenic H^+/K^+ antiporter.

Box 1 | **Proposed role of V_0 in membrane fusion**

Mayer and co-workers have proposed that the V_0 domain, and in particular the DCCD (N, N′-dicyclohexylcarbodiimide)-reactive proteolipid c subunits, have a direct role in membrane fusion[10]. They have identified the formation of *trans*-complexes between V_0 domains in adjacent membranes that shows the same dependence on inhibitors (such as Microcystin) and activators (such as calmodulin) as the fusion process itself. The authors propose that, after SNARE-mediated docking, these *trans*-complexes promote the mixing of the lipid bilayers by virtue of the highly hydrophobic proteolipid subunits. One problem with the model shown is the fact that disruption of the proteolipid genes does not lead to fragmentation of the vacuole in the way that disruption of certain other genes that are involved in this process (such as *VAM3*) does[91,92]. So, the role of V_0 in membrane fusion remains controversial and additional experiments will be required to resolve this question.

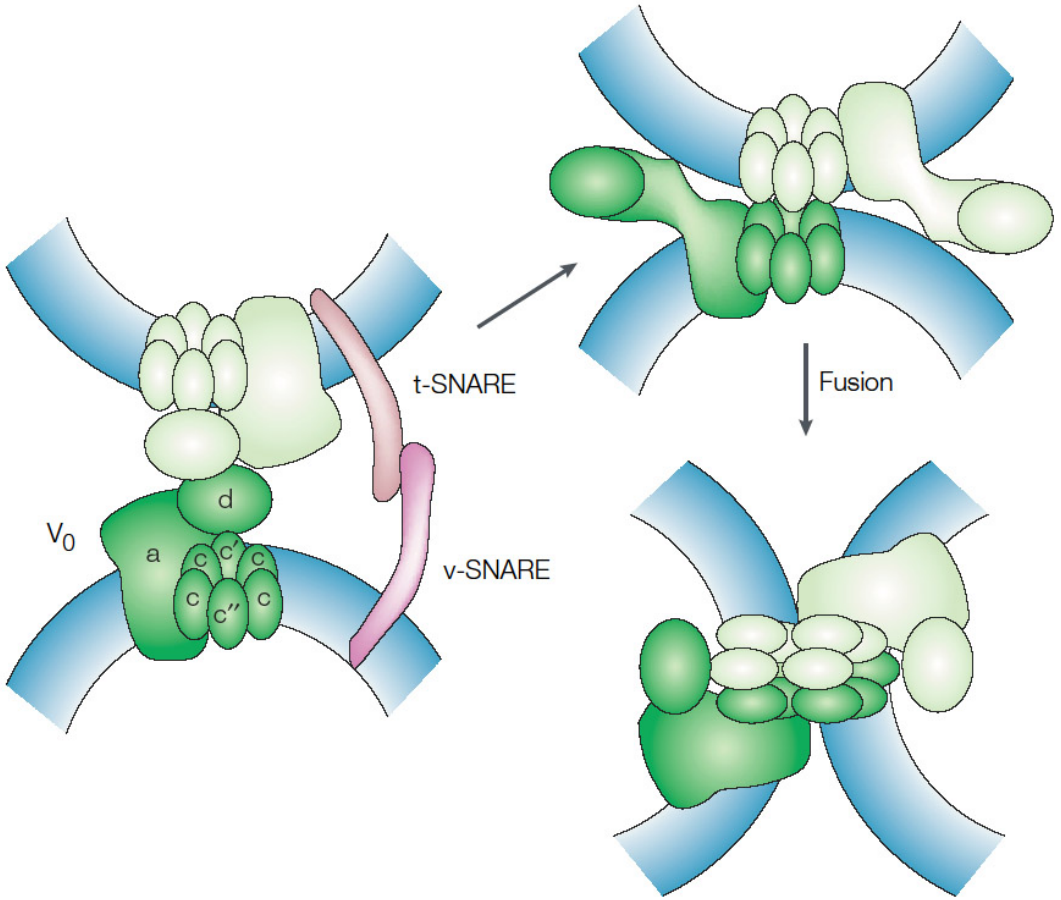

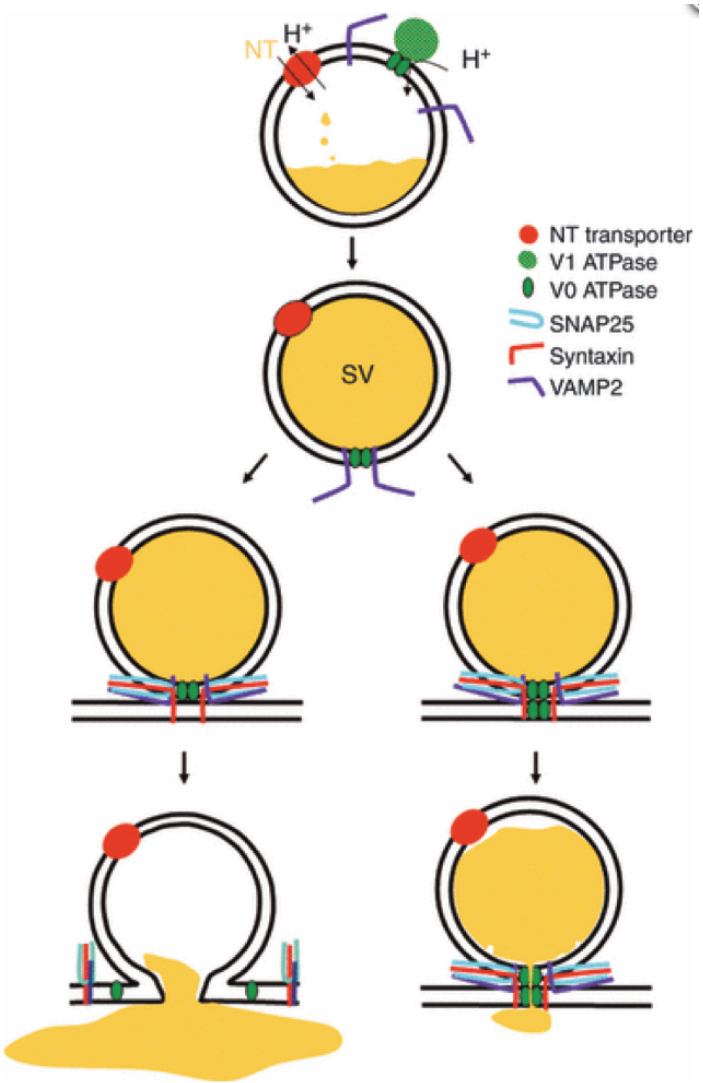

A role for V-ATPase subunits in synaptic vesicle fusion?

Oussama El Far, Michael Seagar

J. Neurochem. (2011) **117**, 603–612.

Figure 1. V-ATPase, synaptic vesicle acidification and hypotheses beyond. ATP-driven H^+ transport through fully assembled V-ATPase at synaptic vesicle (SV) membranes is crucial for synaptic vesicle loading in neurotransmitters (NT). Completion of synaptic vesicle loading may lead to dissociation of the V1 sector and render V0 accessible to bind VAMP2. The c-subunit hexamer (illustrated as two apposed green ovals) assembles a radial array of five to six VAMP2 molecules and could thus act as scaffolding to position an optimal number of v-SNAREs for fusion. (Left) In this pathway, the radial array of v-SNAREs pairs with t-SNAREs and drives fusion mechanically. V0 subunits (single green ovals) disperse laterally in the plane of the membrane during fusion. (Right) SNARE-pairing apposes two V0 sectors to form trans complexes (illustrated as four apposed green ovals). In this configuration, V0 sectors might constitute an aqueous fusion pore. Note that SNARE-binding partners that act at late steps in fusion (e.g. synaptotagmin, complexin….), as well as V0 a- and d-subunits have been omitted to simplify the schema.

The V_O Rotor of the V-ATPase

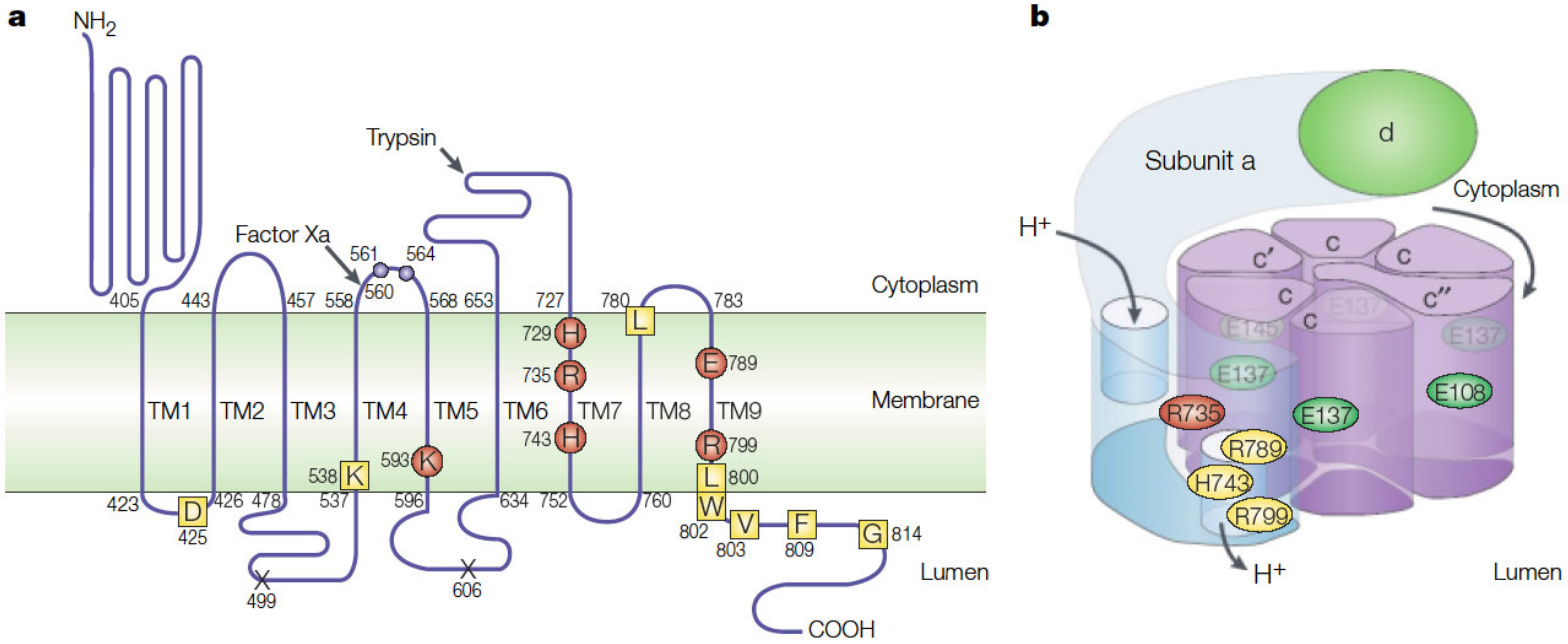

Figure 6 | **Structure and function of the V_0 domain. a** | Topological model for the 100-kDa a subunit based on cysteine-mutagenesis and chemical modification[67]. Residues in yellow are important for assembly, whereas those in red are important for activity. R735 is absolutely required for proton transport[69]. **b** | Proposed structure of the V_0 domain. The proteolipid subunits (c, c′ and c″) form a ring (similar to that of F_0 (REF. 30)) in which each subunit contributes a single essential buried carboxyl group (shown in green) that undergoes reversible protonation. Subunit a is thought to provide access of protons to and from these sites, by analogy with subunit a of the F-ATPases[36,37]. Rotation of the proteolipid ring brings each carboxyl group into sequential contact with the two hemichannels in subunit a, which drives unidirectional proton transport. R735 stabilizes the unprotonated form of the buried carboxyls at the interface of the a and c subunits.

Structure of the Rotor of the V-Type Na^+-ATPase from *Enterococcus hirae*

Takeshi Murata,[1] Ichiro Yamato,[2] Yoshimi Kakinuma,[3] Andrew G. W. Leslie,[4]* John E. Walker[1]*

The membrane rotor ring from the vacuolar-type (V-type) sodium ion–pumping adenosine triphosphatase (Na^+-ATPase) from *Enterococcus hirae* consists of 10 NtpK subunits, which are homologs of the 16-kilodalton and 8-kilodalton proteolipids found in other V-ATPases and in F_1F_o- or F-ATPases, respectively. Each NtpK subunit has four transmembrane α helices, with a sodium ion bound between helices 2 and 4 at a site buried deeply in the membrane that includes the essential residue glutamate-139. This site is probably connected to the membrane surface by two half-channels in subunit NtpI, against which the ring rotates. Symmetry mismatch between the rotor and catalytic domains appears to be an intrinsic feature of both V- and F-ATPases.

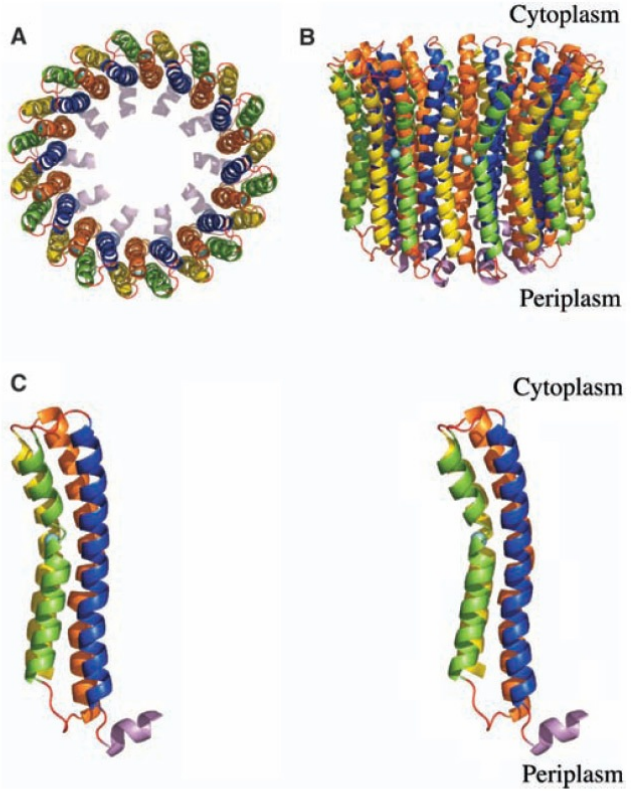

Fig. 2. Structure of the K ring. The ribbon representations are shown in mono (**A** and **B**) and in stereo (**C**). H0 (residues 1 to 8), H1 (11 to 46), H2 (51 to 79), H3 (85 to 124), H4 (127 to 156), and loops (9 to 10, 47 to 50, 80 to 84, and 125 to 126) are colored violet, blue, green, orange, yellow, and red, respectively. The Na^+ ions are shown as light blue spheres. (A) shows a view from the cytoplasmic side of the membrane; (B) and (C) show side views of the K ring and of the monomer, respectively. The cytoplasmic and periplasmic sides of the membrane are indicated.

Different gear ratios

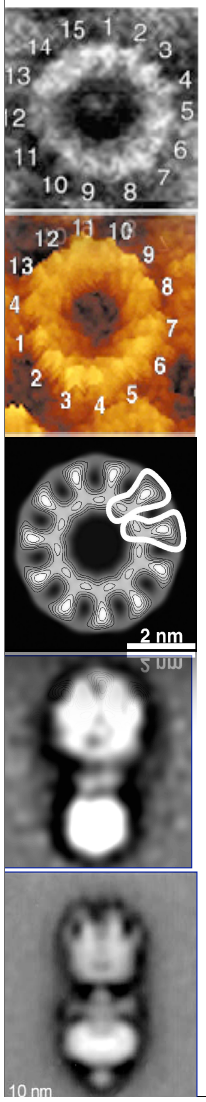

S. platensis F-ATP Synthase:

15 x "high gear"

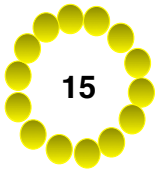

Chloroplast F-ATP Synthase:

14 x "high gear"

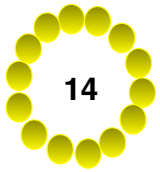

I. tartaricus F-ATP Synthase:

11 x "intermediate gear"

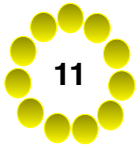

Yeast F-ATP Synthase:

10 x "low gear"

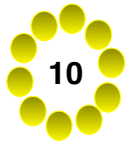

Bovine V-ATPase:

10 x "low gear"

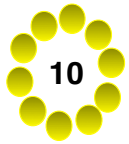

Fixed gear?

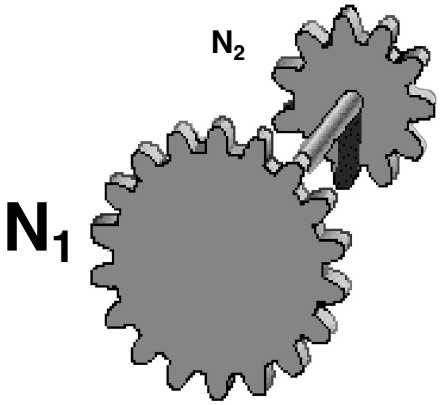

Or variable transmission ?

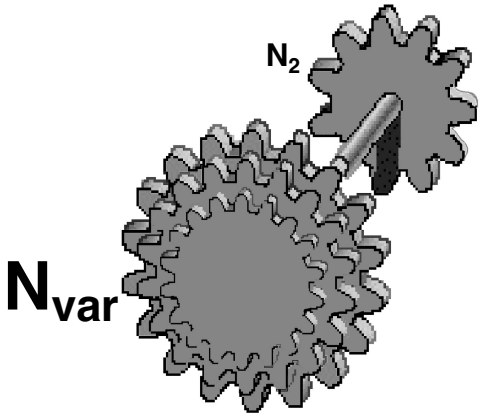

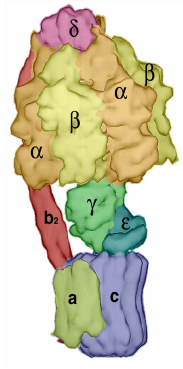

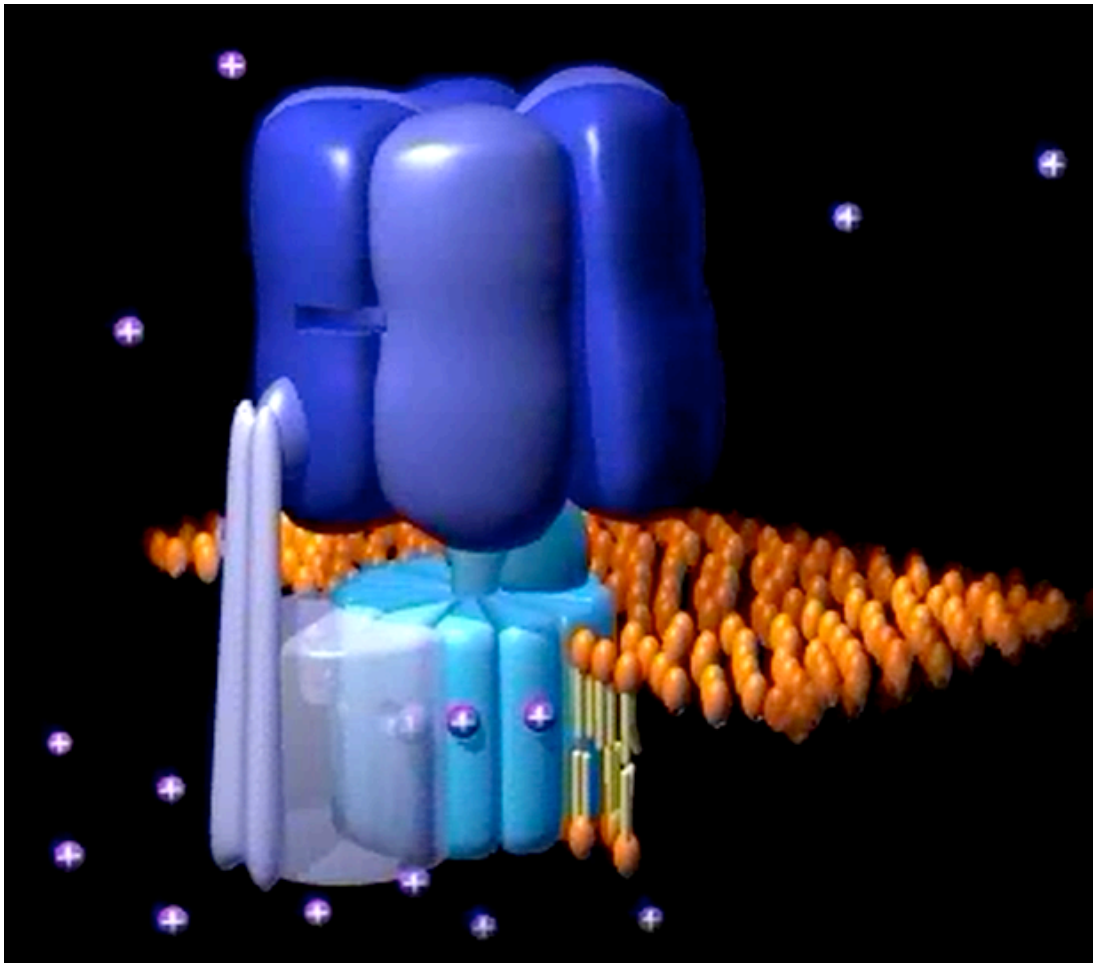

(year ~2000)

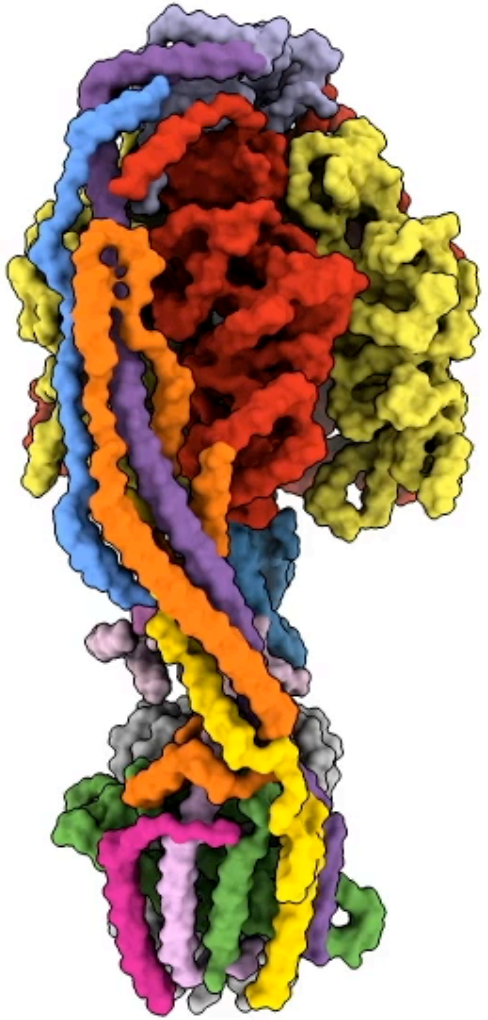

(year 2022)

Structure of ATP synthase under strain during catalysis
Hui Guo, John L Rubinstein
bioRxiv 2022.01.24.477618; doi: https://doi.org/10.1101/2022.01.24.477618